230 (2023) 212156

Contents lists available at ScienceDirect

Geoenergy Science and Engineering

journal homepage: www.sciencedirect.com/journal/geoenergy-science-and-engineering

Literature review on surface-active components in emulsions and foams: Theory and modelling efforts

Galina Simonsen *, Jørn Kjølaas, Paul Roger Leinan, Heiner Schümann

Department of Process Technology, SINTEF Industry, 7034, Trondheim, Norway

ARTICLE INFO

Keywords:
Surface-active components
Emulsions
Foams
Flow behaviour
Coalescence
Separation

ABSTRACT

In this paper we present a literature review on the role of surface-active components in emulsions and foams. Models are presently unable to accurately predict scenarios involving multiphase flows with complex chemistry, and this is a major obstacle for many petroleum production/transport systems. This paper highlights some of the most important physical phenomena that are relevant for understanding and ultimately predicting the flow behaviour of complex fluid systems. Some of the main topics addressed are fluid interfaces with surfactants, droplet coalescence and breakup, emulsions, and foams.

1. Introduction

In this paper we present a literature review on the role of surface-active components in emulsions and foams. In a system of two or more immiscible fluids, entrainment of one fluid phase into the other fluid phase will occur given enough deformation of the fluid interfaces, for example caused by some external force such as shaking of a sealed bottle containing oil and water (Fig. 1). The entrainment process leads to a dispersion where one phase is suspended as droplets or bubbles throughout the other substance producing emulsions (liquid droplets dispersed in an immiscible second continuous liquid), and foams (gas bubbles dispersed in a continuous liquid) for gas-liquid systems. From a thermodynamically point of view these dispersions are unstable, and this instability can be understood by considering the surface energy of the system that arise from the product of the total interface area between the immiscible fluids and the surface tension. An energy minimum exists for a fully separated system of immiscible fluids compared to a dispersed system which has a significant larger total interface area. For a dispersed system, continued coalescence of droplets over time will decrease this potential energy, a process that can be accelerated by external influences, such as gravity, which promote the interaction between droplets. The coalescence process is a result of drainage and rupture of the thin liquid film of the continuous phase separating the suspended droplets. In the case of "clean" immiscible fluid systems (no additives), the coalescence process is normally fast, e.g., in the order of seconds for a mineral oil-water dispersion produced in a bottle shake test. However, the high rate of coalescence for "clean" fluid systems is facilitated by fully mobile liquid film interfaces at the droplet scale. The introduction of surfactants and particles that collect at the interfaces may severely limit or block this mobility and significantly reduce liquid film drainage rate and in some circumstance causing the complete stabilization of emulsions and foams (Fig. 2, Fig. 3). In general, surfactants encompass a large variety of chemicals with different structures, charges, and solubilities. Due to their versatile nature and functionalities, surfactants found a widespread use in a variety of applications where foam or emulsion stability is essential for the final products. Some of the specific examples include food, pharmaceuticals, cosmetics, and detergent production. Furthermore, the concentration of surfactants and interfacial mass transport have major contributions to both formation and stabilization of emulsions and foams. A surfactant adsorbed at internal interfaces will decrease the interfacial tension which play a role in both the formation and stability of the dispersion, e.g., lower surface tension allows smaller droplets/bubbles to be formed during entrainment. Secondly surfactants stabilizing action can be described by two mechanisms, steric and electrostatic, where electrostatic stabilization is characteristic to anionic surfactants which create repulsive interactions at the droplet surfaces which resist the thinning of the liquid film between droplets. In the following sections we will go into greater detail on these phenomena as presented in the literature. This governs the specific effects of different surfactant types, namely non-ionic, anionic, and cationic surfactants.

The focus for this review is fluid systems containing surface active components that cause fluid mixtures to alter their behaviour in flowing systems, and the status of modelling activities on simple macro- and microemulsions and foams are reviewed. Furthermore, the attention is

* Corresponding author.
E-mail address: galina.simonsen@sintef.no (G. Simonsen).

https://doi.org/10.1016/j.geoen.2023.212156
Received 12 December 2022; Received in revised form 16 June 2023; Accepted 13 July 2023
Available online 15 July 2023

List of symbols

Greek

α	droplet collision efficiency
$\dot{\gamma}$	shear rate
$\dot{\gamma}^*$	critical shear rate
Γ	surface excess (surface adsorption)
Γ_{eq}	equilibrium interfacial concentration or surface excess
Γ_f	surface concentration in a thin film
$\Gamma(t)$	dynamic surface adsorption
Γ_{Pb}	surface concentration within the Plateau borders (Pb)
Γ_∞	adsorption capacity
ε	energy dissipation
ε_o	emulsion holdup
E_f	thin film elasticity (also referred to as ε_f/r_f)
η_o	continuous phase viscosity
η_c	continuous phase viscosity
η_{dr}	dispersed phase viscosity (droplet)
η_{em}	emulsion viscosity
θ	contact angle
λ	factor representing the ratio of viscosities of liquids forming the droplet
λ	thickness of the dispersion band
λ_m	viscosity ratio: dispersed phase/emulsion
μ_e	dynamical continuous phase viscosity
Π	disjoining pressure
Π_{edl}	repulsive electrical double-layer forces
Π_s	repulsive steric forces
Π_{vdw}	attractive van der Waals forces
ρ_c	continuous phase density
P_c	Capillary pressure
P_σ	local capillary pressure of the growing local concavity
σ	surface tension or surface tension of a freshly formed interface
σ_{eq}	equilibrium surface tension
σ_o	surface tension of a pure solvent
τ	integration variable
τ_c	characteristic collision time
τ_c	characteristic time describing a quasi-plateau
τ_d	drainage time for droplet-droplet coalescence
τ_d	interfacial coalescence time
τ_I	drainage time for drop-interface coalescence
υ	volume of droplets in the band characterizing their size
υ_g	gas velocity
φ	concentration of dispersed phase
φ_c	concentration of continuous phase
φ_d	concentration of dispersed phase
$\varphi\ (\tau)$	concentration of surfactants in the subsurface layer
ψ_m	maximum interfacial coalescence rate
Ω	foamability number

Roman

A	surface area of a thin film
A	Plateau border area
B_o	Boussinesq number
c	molar concentration of surfactant in the bulk
C	surfactant concentration
C	factor in order of 1 (reflecting the Ca^*)
C_o	bulk surfactant concentration
C_a	Capillary number
Ca^*	critical value of the Capillary number
Ca_m	"mean field" Capillary number
C_H	constant (C_H = O (1))
C_{PR}^{INI}	normalized surfactant concentration
C_s	surfactant concentration at the subsurface
d_{32}	Sauter mean droplet diameter
d_k	characteristic length
D	diffusion coefficient
D	droplet diameter
D	dimensionless factor characterizing the degree of anisotropy
D*	renormalized diffusion coefficient
D_{eff}	apparent diffusion coefficient of a surfactant
D_{max}	maximum droplet size
$D_{TI,max}$	maximum stable droplet size in TI regime
$D_{TV,max}$	maximum stable droplet size in TV regime
E_a	activation barrier energy
f	friction factor
*Gi*Surfactant diffusionG′	Surfactant diffusionG′elastic emulsion component
ΔG	free energy change for the formation of an activated site
h	thin film thickness
H	Hamaker coefficient
H_o	emulsion height
h_{cr}	critical film thickness
k_1	coefficient depending on the ratio of gravity to viscous forces
k_2	coefficient depending on the ratio of capillary suction to viscous forces
K_L	ratio between the adsorption and desorption rate constants
L	DPL thickness
L	impeller diameter
L_o	initial DPL thickness
N_{Vi}	viscosity group forces
N_{We}	Weber group forces
P_b	Plateau borders
ΔP	Young-Laplace pressure
r_a	droplet radius out of contact area
r_V^+	asymmetry parameter (fluid system dependent)
R	droplet radius
Re_{Gs}	surface elasticity modulus
Re	Reynolds number
R_o	mean droplet radius
$R_{n,1}$ and $R_{n,2}$	principal radii of curvature with $R_n = R_{n,1} = R_{n,2}$ for spherical droplets
R_{max} and R_{min}	equatorial radii of a droplet
R_b	P_b length (in the order of the bubble radius)
R_{lim}	limiting droplet radius

directed at systems where surface-active agents or surfactants stabilize or destabilize emulsions or foams. To that end, it is assumed that "stabilizing" an emulsion is equivalent to increasing the coalescence/separation time scales for the droplets, while "destabilizing" an emulsion is to decrease this time scale. Consequently, the key to predicting the behaviour of these complex fluid systems is to predict the droplet coalescence/separation time scales. The matter of droplet coalescence is however profoundly complex and predicting this process from first principles would require modelling of the detailed molecular structure of individual chemical components, which will not be possible in the foreseeable future. Nonetheless, these effects can be very important for predicting flows with surface active components. For instance, in multiphase petroleum production/transport systems, the fluids usually contain either natural surfactants or chemical additives. These fluids are

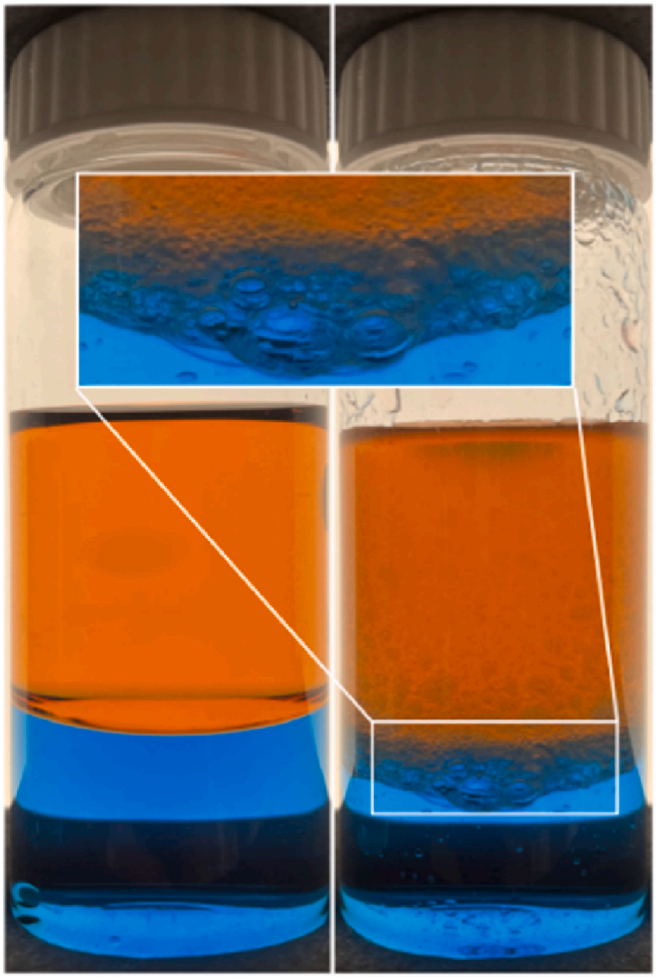

Fig. 1. Bottle emulsion separation shake test of oil (red) and water (blue). Left: fully separated phases before shaking (minimum surface area configuration). Middle: emulation layer of droplets after shaking. Closeup of the emulsion layer showing water droplets in oil.

often exposed to high-shear environments such as pumps and chokes, potentially leading to emulsions with high effective viscosities and subsequently high flow resistance. The total flow resistance in the system will then be a strong function of the stability of the emulsion, since a very stable emulsion may remain unchanged throughout the entire pipe length, leading to a high frictional pressure drop, while a semi-stable emulsion may gradually separate on the way, leading to a lower total frictional pressure drop. It is thus clear that methods for predicting the effect of surfactants and chemicals are needed. In the short term, we believe that progress can be made on the modelling of complex fluid systems by deploying pragmatic fluid characterization techniques, yielding bulk parameters that can be applied in flow simulations. However, to develop such methods, a good overview and understanding of the underlying physics is needed.

In the following sections we provide an overview of some of the most important elements and concepts related to surfactant-rich fluid systems. This governs dispersion systems, namely emulsions and forms in presence of surfactants and particles as stabilizing agents. Section 2 discusses interfacial hydrodynamics and how this affects the behaviour of foams and emulsions. In section 3 we focus on droplet coalescence and breakup, highlighting some of the most applied modelling approaches for these processes, and in section 4 we discuss how these processes relate to the stability of foams and emulsions. In section 5 we outline how surfactants can affect the stability of foams and emulsions, and in section 6 we provide a summary of the most important elements of this literature review.

2. Fluid interfaces

The interface between two immiscible phases can be described as a dividing line of a certain thickness and properties that are different from the properties of the two distinct phases (Tadros, 2013a). A defining characteristic of the interface is that it is in a state of tension and work is required to extend the surface. This surface tension arises from an imbalance of the cohesive forces on molecules of a liquid at the interface compared to the bulk liquid. Surfactant adsorption at liquid-gas and liquid-liquid interfaces has a profound effect on both interfacial tension and overall properties of the respective dispersion systems presented in this review. In the following sections we highlight some of the most important types of interfaces and phenomena to consider when modelling interfacial dynamics.

2.1. Foams and liquid-gas interfaces

Foams are colloidal dispersions, where a gas is dispersed in a continuous liquid phase, and liquid-gas (L-G) interfaces are formed (Schramm, 2005). Foams are created in numerous situations for example in breaking waves; at the discharging into separators; and in gas-liquid pipe flow (Fig. 3a). Foam can be characterized as aggregated gas bubbles in a liquid film network. The shape of the gas bubbles can vary from spherical for wet foams to polyhedral for dry foams. The maximum packing density of spheres, $\varphi_c = 0.36$ (where φ_c is the liquid fraction), defines the limit between bubbly flow and wet foam, furthermore the transition between wet and try foam, at $\varphi_c = 0.01\ldots0.05$, is reached when the gas bubbles premodernity have a polyhedral shape (Cantat, 2018). Foam bubbles vary in diameters within the range of ten to several hundred μm (sometimes ≥1000 μm) and, despite being a polyhedral, typically referred to as spheres with certain diameters (Schramm, 2005).

All foams are thermodynamically unstable. As the continuous liquid phase bounding gas bubbles forms a liquid film with a large surface area which is in a state of tension because of surface tension (σ) forces. Foam stability will depend on the drainage and thinning tendency of the liquid film between the bubbles as well as its possible rupture resulting from

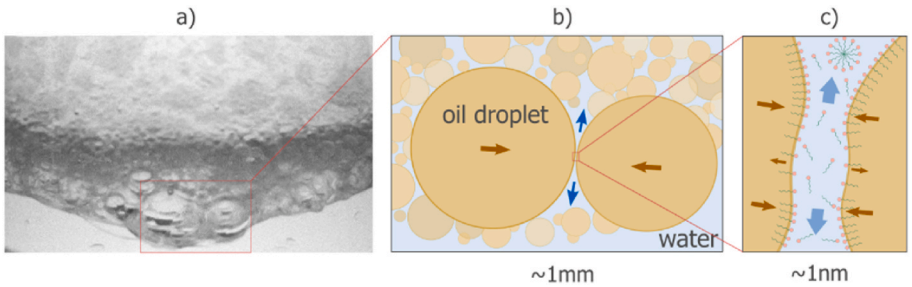

Fig. 2. a) Emulsion layer composed of oil droplets dispersed in water phase. b) Two oil droplets approaching each other. c) Closeup of the area between two droplets filled with surfactant rich bulk phase.

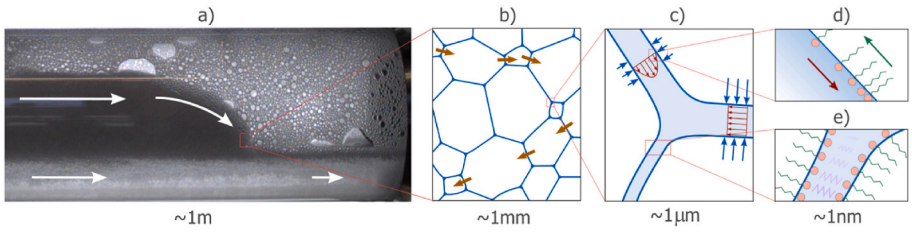

Fig. 3. a) Foamy liquid hydrodynamic slug flow in a 4″ horizontal pipe with surfactants. b) Polyhedral gas bubbles in a continuous liquid film network (dry foam), where the deformation/flow of the foam from propagation and rearrangement of liquid lamellae is illustrated. c) The intersection between gas-bubbles with three liquid lamellae meeting at a Plateau border. Three lamella/Plateau drainage scenarios are illustrated (from the top): drainage with immobile interfaces; drainage with fully mobile interfaces; and arrested drainage. d) Interface immobilised by a gradient in surfactant concentration (Marangoni-Gibbs effect). e) Drainage arrested by disjoining pressure from surfactants in a thin liquid film.

random mechanical action (Nguyen and Schulze, 2003). In most clean systems without surface active additives, film rupture happens fast when the film thickness is drained below a critical values (section 2.3.2) because of the absence of mechanisms/forces opposing the final thinning of the film (e.g., some disjoining forces) below the rupture threshold. The film rupture theory was originally formulated for the case of foams (Sheludko, 1967; Vrij, 1966a). In most cases the thin film will be in contact with the bulk liquid and its drainage is affected by a range of external and internal forces (which are the same forces acting on a film between two droplets in emulsion systems). The capillary pressure of the film meniscus is an external force forcing the liquid out of the film, and the rate of this drainage in clean systems is mainly determined by fluid viscosity. Disjoining pressure (Π) is an internal force creating additional pressure inside the film and disjoining interfaces (Sheludko, 1967). Disjoining pressure covers total interactions across the film between a droplet and a bubble (or two droplets) and is defined by a sum of short-range attracting van der Waals forces (Π_{vdw}), repulsive steric (Π_s), and long range repulsive electrical double-layer forces (Π_{edl}) (Miller and Liggieri, 2011). Equilibrium liquid films are formed under following thermodynamic conditions:

$$\Pi = P_c > 0 \text{ and } \left(\frac{d\Pi}{dh}\right) < 0$$

where P_c is the capillary pressure of the liquid film meniscus and h is the film thickness. Thus, to balance P_c, the disjoining pressure must increase in magnitude as the film thickness decreases. Among other factors influencing foam stability are both evaporation and gas diffusion through the liquid films.

2.2. Emulsions and liquid-liquid interfaces

Emulsions are colloidal dispersions, where a liquid is dispersed in another continuous liquid, and liquid-liquid (L-L) interfaces are formed (Schramm, 2005) (Fig. 4). Emulsions can be classified as nano- (20–200 nm droplets), micro- (0.01–0.2 μm droplets) or fine and macro- (0.2–50 μm droplets) or coarse according to droplet sizes. Emulsions can also, depending on the type of the continuous phase, be of type water-in-oil (W/O) or oil-in-water (O/W). The simplest examples of multiple systems are W/O/W and O/W/O double emulsions. Most emulsions are thermodynamically unstable and tend to coalesce and separate into separate phases. Emulsion colloidal stability is often discussed by the Derjaguin-Landau-Verwey-Overbeek (DLVO) theory, suggesting that the droplet stability against aggregation depends on the balance between van der Waals attraction and electrostatic repulsion (Derjaguin et al., 1987). The DVLO theory does however not cover all forces accountable for the whole variety of relevant interactions, including steric repulsion, depletion attraction, hydration and hydrophobic interactions, oscillatory surface forces, etc. In the case of emulsions, the droplet's internal fluidity[1] and interfacial mobility will also have a strong impact on the emulsion stability against flocculation. To obtain meta-stable emulsions

[1] Droplet's internal fluidity is a thermocapillary flow inside a droplet.

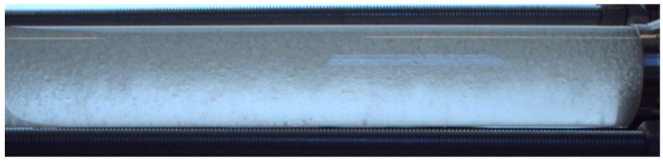

Fig. 4. Fully dispersed emulsion in a horizontal pipe (picture from KPN NEXFLOW).

with oil and water (e.g. mineral oil model emulsions, food, or paints), surface-active agents contributing to reduction of surface tension need to be added (e.g. surfactants, macromolecules, or fine solids) (Milton and Kunjappu, 2012).

Crude oil emulsions are complex fluids systems that have been extensively studied over the past decades and are considered to be stabilized/destabilized with both production chemicals and a variety of naturally present surface-active components including asphaltenes, resins, naphthenic acids, and solids (Berridge et al., 1968; Schubert and Armbruster, 1992a; Tadros, 2013b). Among other factors favouring for example W/O emulsion stability, are high bulk phase viscosity and relatively small volume fractions of the dispersed phase (Auflem, 2002). Properties of an oil phase capable of forming mesostable emulsions (separating within 1–3 days) with water were, as identified by Fingas and Fieldhouse (2003): a viscosity in the range 6–23,000 cP, an asphaltene content of 3–17%, a resin content of 6–30%, asphaltene – to - resin ratio 0.47, an average increase in apparent viscosity by 45 cP at a day of emulsion formation and 30 cP a week later. To form stable emulsions (meaning no separation for at least 4 weeks), following criteria have to be fulfilled: a viscosity in the range of 15–10,000 cP, asphaltene content of 3–20%, a resin content of 5–30%, asphaltene – to - resin ratio of 0.74, an average increase in apparent viscosity by 1100 cP at a day of emulsion formation and 1500 cP a week later. This underscores the importance of asphaltene – to - resin ratio effect on expected emulsion stability.

A special case of extremely stable emulsion that may not separate for months is a dense-packed layer (DPL) (Hartland, 1979). It forms and accumulates at the oil-water interfaces in separators and pipelines used for crude oil emulsion transport. The same is valid for mineral oil emulsions typically used as model fluids to mimic behaviour of the real systems (Fig. 5). The DPL acts as a sort of "fluidic filter" accumulating smallest droplets from separating emulsion. According to different sources, a DPL formed in separators can be divided into 2 or 3 zones (upper, middle, and lower) depending on emulsion type, water percentage, and dominant stabilization components (Borisevich and Krasnova, 2010). In the upper layer, water content is in the range of 30–50%. In the lower layer, it reaches 90%. The amount of water primarily depends on the temperature of the dehydration process. In crude oil emulsions, DPL thickness generally increases with increasing contents of paraffins, asphaltenes, iron sulphides, and solids. Paraffinic compounds become dominant stabilizers at temperatures around 5 °C and are not affected by pH of the emulsified water. Certain production chemicals may also build up gel-like particles acting as stabilizers. pH of the

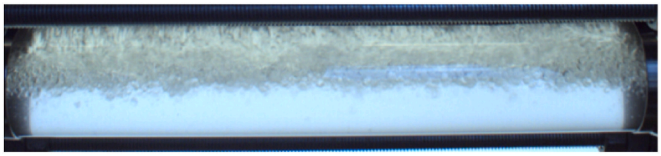

Fig. 5. DPL formation in a horizontal pipe (picture from KPN NEXFLOW).

emulsified water has significant effect on DPL stability (Karpenko and Konovalov, 2019).

2.3. Physicochemical hydrodynamics of thin liquid films (L-G and L-L interfaces)

2.3.1. Rate of drainage of thin liquid films

The process of droplet-droplet coalescence involves drainage of the film separating the droplets. The coalescence time scale depends on how fast this film is drained, and coalescence is understood to occur when the film thickness drops below some threshold. Various factors including system chemical composition and surfactants (and their local arrangements and concentration gradients), bulk viscosities, surface tension, surface dynamic viscosity, and surface elasticity will influence the rates and times of thin film thinning. The non-homogeneity of the film thickness also shortens the time of film rupture. The film non-homogeneity increases with the droplet radius. Surface tension for clean systems, such as pure water and air, is typically (may change with temperature) constant and independent of the change in the surface area. Thus, films composed of clean phases typically survive less than 2–6 s and do not exhibit a measurable pattern of thinning[2] (Velikov et al., 1997). The important contribution of the surfactant effect on the rate of drainage of liquid films has been extensively studied by the group of Ivanov (Radoëv et al., 1974). One of the effects is associated with the hydrodynamic flow, that is driving the adsorbed surfactant molecules away from the film centre as the gradient of adsorption (the Marangoni-Gibbs effect) tends to restore the equilibrium and restricts film drainage (Radoëv et al., 1974). Ivanov and Traykov later predicted that the drainage of interfacial films between two droplets happens much faster when the surfactant is dissolved in the dispersed phase (Traykov and Ivanov, 1977). A formula for the velocity of film thinning was derived. It was concluded that the velocity of thinning of emulsion films differed only slightly from that for foam films when the surfactant was soluble in the dispersed phase. This provided a hydrodynamic explanation of the empirical Bancroft rule, stating that "in order to have a stable emulsion, the surfactant must be soluble in the continuous phase" (Ivanov and Kralchevsky, 1997).

The surfactant effect is closely related to the practically important hydrodynamic stability of foams and emulsions. Lifetimes of foam films stabilized by two ionic surfactants were measured and showed remarkably good linear relationship to the surfactant concentration logarithm at a wide concentration range. The drainage velocity typically slows down with a decrease of the film thickness. From the values of the capillary pressure P_c, the film elasticity ε_f/r_f and the contributions of the disjoining pressure Π (under a set of selected values of parameters), the drainage velocity of the thin film can be calculated using modified Reynolds–Scheludko equations (Sanfeld and Steinchen, 2008). The film thickness velocity for small droplets (1.53 μm) with higher surface tension (17 erg/cm^2) is larger than the film thickness velocity for droplets with low surface tension (3 erg/cm^2).[3]

According to work of Henschke et al., drainage times for drop-interface and droplet-droplet coalescence can be calculated as (Henschke et al., 2002):

$$\tau_I = \frac{(6\pi)^{\frac{7}{6}}\eta_c r_a^{7/3}}{4\,\sigma^{5/6}\,H^{1/6} r_{F,I} r_V^{+}}$$

where the Hamaker coefficient H is in the power of 1/6 and, thus, its value does not significantly affect the results. It can be fixed at 1×10^{-20} *Nm*, while the asymmetry parameter r_V^+ depends on the fluid system.

2.3.2. Critical thickness of thin liquid films

Scheludko's theory states that the liquid film reaches upon thinning the state of kinetic instability and then, due to spontaneously growing thermal fluctuations (surface waves), collapse of the film occurs at its critical thickness (Scheludko, 1962). This collapse leads to the event of droplet or bubble coalescence. The Scheludko's criterion gives the condition for this critical translation from metastable to spontaneously growing surface wave amplitude:

$$\frac{d\,\Pi}{d\,h} = \frac{d\,P_\sigma}{d\,h}$$

where P_σ is the local capillary pressure of the growing local concavity, h is the film thickness and Π is the additional (disjoining) pressure. The equation is applicable for small film radii of <0.05 mm.

The **Radoev–Scheludko–Manev model from 1983** (applicable to larger film radii) described a new theoretical approach concerning the film destruction or "black spot formation" (Radoev et al., 1983). It yielded a new more general formula describing quantitatively Scheludko's criterion and considering the effect of the film's thickness local inhomogeneity. It was, however, established later that a different mechanism of film rupture could occur as a result of solute transport across the liquid film and appearance of the Marangoni instability (Dimitrova et al., 1988).

2.3.3. Thin film elasticity

The theory of film rupture formulated for foams is, with a slight modification, applicable for films in emulsions (Ivanov and Traykov, 1976). It is suggested that the true stability of the liquid films is related to their thermodynamic properties, i.e. surface tension and disjoining pressure. As for the coupling of hydrodynamic properties and mass flow of surfactants at the interface, it is closely related to the time evolution of the film drainage, which can be expressed by the interfacial mobility of thin liquid layer alone. The interface with adsorbed surfactant layers will vary in thickness, density, and rheology depending on the molecular dimensions, surface loading, and interactions between the surfactant molecules. While the lifetime of the films is strongly affected by the interfacial mobility, the thickness of rupture is dependent on the mobility factors. Several mechanisms have been proposed for the final rupture of a thin film and it is generally accepted that the film rupture occurs due to instabilities arising in the interfacial regions caused by surfactant concentration or temperature gradients. The surfactants tend to accumulate at the L-L interfaces and reduce interfacial tension. As emulsions are dynamic systems, bulk fluid motion or flow disturbs homogeneity of the molecular composition at the interfaces. This creates a local interfacial tension gradient attempting to restore to its equilibrium state – a process that also creates a flow. That flow is known as Gibbs-Marangoni effect and it plays a role in returning the thin film to its original shape. The resistance to surface deformation can be expressed in terms of the surface elasticity. For the L-L or L-G interfaces, the film elasticity can be expressed as (Christenson and Yaminsky, 1995; Ata et al., 2011):

$$E_f = -2\,\frac{d\sigma}{d\,(\ln A)} \quad \text{or} \quad E_f = \frac{4c\,(d\sigma/dc)^2}{kTD}$$

where E_f is the elasticity, A is the surface area of a film, D is the sur-

[2] Impossible to observe typical stages of film thinning.

[3] An erg is the amount of work done by a force of 1 dyne exerted for a distance of 1 cm: 1 erg = 1.000000 × 10^{-7} J.

factant diffusivity, k is the Boltzmann constant, T is the temperature, and c is the surfactant concentration on the film surface. The second equation is derived from the first by introducing the Gibbs absorption equation, and it underscores that the source of the surface elasticity is that a change in surface area will yield a change in the surfactant concentration, which subsequently leads to a change in the surface tension.

2.4. Surfactant interfacial transport and adsorption

Surface tension of a freshly formed interface (σ) is close to that of a pure solvent (σ_o). It will continuously decay over time until reaching the equilibrium (σ_{eq}), the process known to take milliseconds to days for different systems. The interfacial concentration or surface excess of a surfactant solution at equilibrium is given by Γ_{eq}. The surface adsorption is driven by adsorbing and desorbing fluxes of surfactant molecules to and from the surface and is a dynamic process. As a droplet or a bubble is formed, the surface excess (Γ) (which can be calculated from the Gibbs adsorption isotherm equation) will become smaller than the Γ_{eq}. In this case, the system will try to return to the equilibrium state by creating a higher adsorbing surfactant molecule flux (Eastoe and Dalton, 2000). The surfactant transport at the interface can be described by several models, including two examples presented here: a diffusion control model and a mixed diffusion-kinetic) (Eastoe and Dalton, 2000; Liu and Messow, 2000).

The diffusion control model is based on the classical 1946 model by Ward and Tordai governing the diffusion of molecules from the bulk to the interface and back diffusion from the interface to the bulk as the interface becomes saturated (Ward and Tordai, 1946). The original equation assumes that every simple molecule arriving at the interface is likely to arrive at an empty site:

$$\Gamma(t) = \sqrt{\frac{D}{\pi}}\left[2C_o\sqrt{t} - \int_o^t \frac{\varphi(\tau)}{\sqrt{t-\tau}}\, d\tau\right]$$

where $\Gamma(t)$ is the dynamic surface adsorption, D is the diffusion coefficient, C_o is the bulk surfactant concentration, t is the time, $\varphi(\tau)$ is the concentration of surfactants in the subsurface layer and τ is the integration variable.

In the diffusion control model, the time scale of adsorption from the subsurface (imaginary plane near the actual L-G interface) to the interface is very fast and the diffusion from the bulk to the subsurface is the rate controlling step. When the Ward and Tordai equation is solved by Laplace transformation, dynamic surface adsorption for short and long time limit adsorption can be calculated:

$$\Gamma(t) = 2C_o\sqrt{\frac{Dt}{\pi}} \text{ and } \Gamma(t) = 2\sqrt{\frac{D}{\pi}}\left[(C_o - C_s)\sqrt{t} + C_s\sqrt{t_1} - \frac{1}{2}\int_0^{t_1} \frac{\varphi(\tau)}{\sqrt{t_1-\tau}}\, d\tau\right] \quad (t \geq t_1)$$

where t_1 is a certain long time at which the concentration at the subsurface has reached a constant value of C_s..

As the L-G interface is strongly curved, interface curvature plays an important role in the adsorption calculation. A spherical interface is characterized by larger ratios of the surface area of a bubble to the volume surrounding it, meaning that more molecules per unit area are available near a spherical interface compared to planar. It has been suggested that the bubble radius at which interface curvature effects become significant, shall be estimated for individual surfactant systems (Alvarez et al., 2010). The equations for adsorption at spherical interfaces for both short and long time limit adsorption are also published by the authors of the diffusion control model (Liu et al., 2004). At the same time, the dynamic surface tension for spherical interfaces at short and long time limit adsorption can be calculated by combining the abovementioned equations with the Gibbs equation and the Langmuir isotherm equations (Liu et al., 2004).

The mixed diffusion-kinetic model describes the molecular diffusion from the bulk to the subsurface as in the diffusion control model, but the rate controlling process is the transfer of the molecules to the interface. It is said that the instantaneous adsorption at the L-G interface might be delayed due to potential energy barriers, molecular reorientation before adsorption, absence of an available site and micellular presence (Eastoe et al., 1998; Poptoshev and Claesson, 2002; Danov et al., 1996). Liggieri and Ravera modified the Ward and Tordai equation by introducing a renormalized diffusion coefficient (D*), taking into account both diffusion to the subsurface and crossing a potential barrier (Ravera et al., 1993):

$$D^* = Dexp\left(-\frac{E_a}{RT}\right) \text{ or } D^* = Dexp\left(-\frac{\Delta G}{RT}\right)$$

where E_a is the activation barrier energy and ΔG is the free energy change for the formation of an activated site. According to the model, only the subsurface molecules with energy greater than E_a will be adsorbed at the interface. Even a small increase in the E_a may correspondingly cause a significant decrease in the adsorption and especially in the long time limit case.

3. Droplet coalescence and breakup

The stability of foams and emulsions is an extremely intricate and complex phenomenon, where predicting coalescence of two droplets or bubbles can be a useful starting point. In fact, understanding the thin film rupture is an important precursor to understand the overall stability of a system. As two droplets approach each other, a hydrodynamic interaction builds up leading to a weak deformation of the front parts of droplets. This causes the interface curvature to be shaped into a concave lens shaped dimple. As the attraction forces overcome the energy barrier created by increase of surface energy during deformation, an outflow of fluid from the dimple will cause the size of the dimple to decrease. This leads to formation of a plane thin liquid film. Usually, the film formation between two droplets is followed by drainage, reducing its thickness (Sheludko, 1967).

It is commonly accepted that foam and emulsion separation may occur as a result of the four different mechanisms.

1. Creaming or sedimentation is a result of a density difference between the two immiscible phases. In the case of an O/W emulsion, the oil droplets will accumulate at the top and form a cream layer.
2. Flocculation is caused by the droplets aggregating due to the presence of a minimum in the interaction energy. The individual droplets remain separated by the thin liquid film. Flocculation enhances creaming and is often a prerequisite step to coalescence.
3. Coalescence is the merge of two or more droplets resulting from breakage of the thin liquid film, which ruptures under the action of attractive forces or hydrodynamic instabilities (Ivanov and Traykov, 1976). It can be followed by coagulation which is the gradual precipitation of droplets as they increase in size.
4. Ostwald ripening is a process of molecular diffusion transfer from a smaller droplet or a bubble to the larger droplet or bubble. The processes driven by chemical potential differences. As described by Laplace, larger bubbles have smaller curvature and, therefore, lower pressure than the small bubbles.

3.1. Droplet-droplet coalescence

Coalescence takes place when droplets collide and merge. The thin film drainage time and the neck expansion comprise main stages of the occurring coalescence mechanism. Despite the significant progress in investigation of the thin film properties, not much information is

available about coalescence rate in real emulsion systems. Multicomponent mixtures of crude oil specific surface-active agents and other factors, including emulsification conditions, temperature, pressure, and pH, make it difficult to evaluate each single contribution and predict emulsion and foam stability. These real systems also manifest a nonlinear dynamic viscoelastic response accompanied by memory effects. The same behaviour is most likely characteristic for coalescence, where the thinning and rupture of the thin films happens beyond the linearity-range limit. This creates the need for experimental studies of complex real systems and better understanding of the combined effects to develop better models.

The drainage times for droplet-droplet coalescence can be calculated as:

$$\tau_d = \frac{(6\pi)^{\frac{7}{6}} \eta_c r_a^{7/3}}{4\,\sigma^{5/6}\,H^{1/6} r_{F,I} r_V^{+}}$$

which is the same equation that can be used to calculate drainage times for drop-interface coalescence (Henschke et al., 2002). Both coalescence times can be used as closures for emulsion separation models. Once the film between two droplets drains to an infinitesimal thickness, the intermolecular forces become dominant and rupture the film. A connecting neck is formed, and its expansion dynamics are controlled by the Young-Laplace pressure (REF):

$$\Delta P = \sigma \left(\frac{1}{R_{n,1}} + \frac{1}{R_{n,2}} \right)$$

where $R_{n,1}$ and $R_{n,2}$ denote the principal radii of curvature with $R_n = R_{n,1} = R_{n,2}$ for spherical droplets. It has to be mentioned that the neck expansion dynamics will, to a large extent, be affected by presence of surfactant molecules adsorbed at the coalescing interfaces and creating a gradient of interfacial tension.

As seen from the equation above, **prediction of droplets sizes** is highly important for accurate prediction of droplet deformation, breakup, and coalescence. Coalescence timescales when two droplets of certain size meet are of particular interest. Some studies experimentally confirm that the larger the droplet diameter, the more stable the droplets are against coalescence. While others mention that larger droplets burst faster than the smaller ones. The explanation here could be given by hydrodynamic regimes of thinning of the neck region, which are affected by e.g., non-uniformity of surfactant distributions and/or differences in viscosities or densities of the fluid systems. However, it seems that coalescence timescales are dependent on the droplet size distributions (polydispersity) as expressed through a change in the functional dependence of the droplet lifetime on its radius. The majority of studies, however, agree that small (μm size) droplets are more unstable when their radius is larger. Just the opposite is the case of big droplets (above 300 μm): the lifetime increases with the size (Basheva et al., 1999).

3.2. Droplet deformation and elongation

Deformation and elongation (transition from spherical to ellipsoidal shape) are processes preceding droplet break-up. Types of droplet deformation and their deformation in flow have been extensively studied with both experimental and modelling techniques (Renardy, 2007a). The driving forces of deformation are shear stresses acting on a droplet, while interfacial tension is the resistance force supporting the shape of a drop and restoration to the original shape. It is well known that low interfacial tension is one of the major causes for deformation of droplet shape. The degree of deformation on the droplet length scale is governed by the capillary number:

$$C_a = \mu_e U/\sigma$$

where μ_e is the dynamical continuous phase viscosity, U is the characteristic velocity of the flow relative to the droplets, and σ is the constant surface tension (the effects of surface tension gradients due to changes in surfactant concentrations or temperature variations are not included). The morphology of a droplet or its elongation is characterized by a dimensionless factor, the degree of anisotropy:

$$D = \frac{R_{max} - R_{min}}{R_{max} + R_{min}}$$

where R_{max} and R_{min} equatorial radii of a droplet.

Taylor's theory of droplet deformation is predetermined by a generalized Weber group. He studied a single drop as a function of the maximum velocity gradient in the flow field, where the only intrinsic length scale is the undeformed droplet radius. In this case (with further assumptions of Newtonian fluids and absence of surfactants), the two non-dimensional parameters governing droplet shape and stability are the ratio of shear and interfacial stresses, expressed by the capillary number C_a. The fundamental linear approximation for calculating the degree of droplet anisotropy is based on the Taylor's model for the viscosity of dilute emulsions and is expressed as (Taylor, 1934):

$$D = \frac{16 + 19\,\lambda}{16\,(\lambda + 1)}\, C_a$$

where λ represents the viscosity ratio of dispersed to continuous phase. Droplet anisotropy for moderately concentrated emulsion droplets can be calculated as follows (dynamic interactions between drops are considered):

$$D = \left[\frac{16 + 19\,\lambda}{16\,(\lambda + 1)} \right] \left[1 + \frac{5\,(2 + 5\,\lambda}{4\,(\lambda + 1)}\, \varphi \right] C_a$$

where φ is the concentration of dispersed phase. Deformation of droplets in flow is by large extent determined by the viscosity of the continuous phase. This was established through an inverse calculation of the fluid viscosity from monitoring the shape of a surfactant-stabilized droplet in flow (Megias-Alguacil and Windhab, 2006). Droplet deformation in a viscous fluid flow is another complex case. One of the most complete solutions includes contributions of all factors influencing droplet shape (including interfacial tension). In this study, droplet anisotropy is calculated from the earlier described Taylor's model for the viscosity of dilute emulsions and compared with experimental data (Jackson and Tucker, 2003).

The majority of publications considers droplets either as being spheres or focus only on the intermolecular and hydrodynamic interactions inside the thin film between them. This neglects the role of the spherical parts of the droplets outside of the zone of flattening. In real emulsions droplets of the same size can be either spheres or be flattened with the intervening film. Even when there is a planar film, the spherical parts of the droplets outside it can play a substantial role for the droplet interactions and overall emulsion stability. Occurrence of flocculation in an emulsion is significantly affected by the droplet deformation in the zone of contact between two droplets (Ivanov et al., 1999). In 2003, Jackson and Tucker presented a model for large deformation of an ellipsoidal droplet with interfacial tension (Jackson and Tucker, 2003). The model considers that both fluids are of Newtonian nature. It allows any value of viscosity ratio but did not incorporate droplet breakup or coalescence. The model was verified using experimental results from the literature including steady shapes in simple shear, transient shapes during shear reversal, widening in simple shear, relaxation after step shear, and the critical capillary number for breakup in both shear and planar elongation. It must be mentioned that in predicting emulsion stability, it is important to precisely determine the range of the droplet sizes and flow conditions, where droplet deformation has an inhibiting effect on droplet coalescence. In the meantime, droplet deformation and elongation will also affect overall emulsion viscosity (briefly described under 5.2) (Torza et al., 1972).

3.3. Droplet breakup

3.3.1. Extensions of Hinze's correlations

The possibility of droplet breakup is governed by whether external stresses exceed forces stabilizing droplet shape. The forces involved in droplet deformation and breakup are thought to comprise two dimensionless groups, a Weber group N_{We} and a viscosity group N_{Vi}. The breakup will occur when group N_{We} exceeds its critical value, $(N_{We})_{crit}$. It was theoretically shown that $(N_{We})_{crit}$ depends on N_{Vi} but also on the patterns of relative velocity variation over time (Hinze, 1948). In 1955, Hinze specified the importance of efficient droplet dispersion as he described three detailed cases of droplet deformation and breakup, including that in a simple viscous flow, that in an air flow, and that in a turbulent flow (Hinze, 1955). The article is based on the earlier experimental studies by Taylor (1934), Lenard (1904), and Clay (1940), respectively. All the cases are thought to arise from different dispersion mechanisms, explaining differences in the $(N_{We})_{crit}$. Thus, experimentally obtained $(N_{We})_{crit}$ values for one dispersion process may, therefore, not be applicable to other processes. $(N_{We})_{crit}$ depended on the type of droplet deformation and on the flow pattern around it. Droplet breakup was shown to be significantly influenced by the density differences between dispersed and continuous phases (valid for both L-L and L-A interfaces). A formula for the maximum droplet size in emulsion was derived:

$$D_{max}\,(\rho_c/\sigma)(\hat{3})\ /\ (\hat{5})\ \varepsilon^{2/5} = 0.725 \text{ (with a standard deviation of 0.315)}$$

where ρ_c is a continuous phase density, σ is interfacial tension and ε is the energy dissipation. It was assumed that the average size of the largest droplet in the field corresponds to the average energy input across this field and that $D_{max} \sim D_{95}$, which is the value for which 95% of volume is contained in the droplets with D < D_{95} (Clay, 1940).

Assuming homogeneous and isotropic turbulence in a pipe, Hinze's correlation was modified through using the mean rate of energy dissipation expressed in terms of a friction factor (Brauner, 2001):

$$\left(\frac{D_{max}}{D}\right)_o = 0.55\left(\frac{\rho_c\, U_c^2 D}{\sigma}\right)^{-0.6}\left[\frac{\rho_m}{\rho_c(1-\varepsilon_d)}f\right]^{-0.4}$$

where f is the Fanning friction factor. The equation is based on a single drop in a turbulent flow and can only be applicable to dilute emulsions. For concentrated emulsions, a new modification of Hinze's correlation was proposed based on an energy balance between the turbulent kinetic energy of the continuous phase and the surface energy produced from the dispersed phase (Brauner, 2001):

$$D_{max} = 2.22\, DC_H^{3/5} We_c^{-3/5} f^{-2/5}\left(\frac{\rho_m}{\rho_c\,(1-\varphi_d)}\right)^{-2/5}\left(\frac{\varphi_d}{1-\varphi_d}\right)^{0.6}$$

where C_H is a constant (C_H = O (1)).

3.3.2. Critical value of the capillary number

Another approach is to consider a critical value of the Capillary number (Ca^*) as the determining factor for droplet stability. This follows from theoretical calculations and experimental data and depends on the ratio of viscosities of the droplet and continuous phase ,λ. The following quantitative approximation at small λ values is proposed (Hinch and Acrivos, 1979):

$$Ca^* = 0.054\,\lambda^{-2/3}$$

Grace (1982) determined that some minimal limit of Ca^* = 0.4 corresponds to the fluid systems of equal phase viscosities (droplet/continuous phase), λ = 1. It was also demonstrated that droplets will not breakup in laminar flow at $\lambda > 4$ (case of high droplet viscosity) (Grace, 1982). In turbulent flow, however, the situation is different as the local flow velocity varies chaotically.

The critical conditions for droplet breakup will however change when the continuous phase is not viscous but viscoelastic. Surface stresses at the interface can vary and are a function of the Reynolds and the Weissenberg numbers (the latter is the ratio of characteristic times of outer action and inner relaxation). It is demonstrated numerically that the Ca^* increases with increasing Weissenberg number (Renardy, 2007b).

4. Modelling of droplet coalescence and breakup (emulsion and foam stability)

The outcome of two droplets or an interface of a fluid body and a droplet colliding depends significantly on the impact of velocity. At high impact velocity, splashing, bouncing (example of non-coalescence), coalescence, partial coalescence (formation of a daughter droplet), temporary coalescence and even droplet fragmentation may occur. If colliding with an interface of a fluid body at low velocities, a droplet may continue resting on a reservoir without coalescing for up to a few seconds. The complexity of the processes and mechanisms occurring in emulsion flow or in foam systems makes it difficult to predict their stability. Thus, certain dominant contributions must be preselected in order to produce reliable predictions. Some of the dominant factors can be flow regimes (affecting velocities of the droplets and bubbles), type and concentration of surfactants, viscosities of the phases, or presence of particles. As some of these parameters are relatively easy to estimate, effects of multicomponent surfactant mixtures possibly combined with fine solid particles generate uncertainty, which is especially relevant for the crude oil production and processing. Surfactants and mixing conditions will significantly affect droplet sizes and size distributions. Dispersed phase fraction and generated droplets of certain stability will, in turn, affect overall stability of the system.

4.1. Foams

Terms steady pneumatic[4] and dynamic[5] foams are typically distinguished for modelling purposes (Bhakta and Ruckenstein, 1995; Exerowa and Kruglyakov, 1997). Ruckenstein's model for predicting foam stability is one of the most elaborate ones (Ruckenstein and Bhakta, 1996; Bhakta and Ruckenstein, 1997). The model predicts the effects of surfactant and salt concentrations on the drainage and collapse of foams. It is shown that both parameters strongly influence the surface viscosity via surface adsorption Γ and hence affect the foam drainage. Neethling's and Grassia's models predict foam stability as a whole (Grassia et al., 2006; Neethling et al., 2005). In a foam with steady uniform bubble size, liquid volume fraction ε, and where Plateau border area A[6] are directly to a proportionality constant in the order of the inverse square of bubble radius, the following foam drainage equation was deducted:

$$\frac{\partial A}{\partial t} + \frac{\partial}{\partial y}\left(\left(-k_1 A - \frac{k_2}{\sqrt{A}}\frac{\partial A}{\partial y} + v_g\right)A\right) = 0$$

where v_g is the gas velocity, k_1 is a coefficient depending on the ratio of gravity to viscous forces, and k_2 is a coefficient depending on the ratio of capillary suction to viscous forces. While these models comprise the main processes governing foam stability, a uniform surfactant distribution is assumed within the foam. As the surfactant concentration can be non-uniform and evolves over time, foam stability models should include conservation laws for surfactant transport.

[4] Pneumatic foams are produced by a continuous stream of gas bubbles rising to the surface of a foaming liquid. Pneumatic steady foams are those under steady-state conditions.

[5] Dynamic foams are those under hydrodynamic conditions.

[6] Plateau borders are channels formed where the thin films from the lamella meet. Plateau border area A is a total cross-sectional area of Plateau borders in a foam.

4.1.1. Surfactant accumulation in the top foam layer

Coalescence within the top layer of foam bubbles can be considered as one of the most important mechanisms in evaluating overall foam stability. The process comes along with surfactant accumulation in the top foam layer (Dukhin et al., 2008). The interface of a bubble formed near the bottom layer will adsorb surfactants from that layer as the rising bubbles convectively transport surfactants to the upper layers (Fig. 6). This leads to surfactant accumulation in the top layer and higher stability of the top layer, promoting stabilization of the foam as a whole (Bikerman, 1953). Thin films rupturing within the top foam layers could lead to a local surfactant accumulation with similar effect on the overall stability (Arbuzov and Grebenshchikov, 1937). Once the surfactant concentration within a dry foam[7] increases in comparison with the initial surfactant concentration, the bulk concentration and the surface concentration (Γ_{Pb}) within the Plateau borders (P_b) are higher than in the film (Γ_f). This leads to reduction of surface tension at the boundary between P_b and the film, which then becomes lower than the surface tension in the film centre. Differences in surface tension contribute to a rise in Marangoni flow towards the thin film and retardation of the film's drainage. It has to be mentioned that the surfactant accumulation in the top layer practically stops when the critical micelle concentration (CMC) is reached (strong downwards surfactant flow contradicts convective upward flow).

An equation for local increase of surfactant concentration as result of thin film rupture was derived by Dukhin et al. and is based on a 2D approach (Dukhin et al., 2001):

$$\frac{\Delta C}{C_o} \approx \frac{3\,\Gamma_o\,C_o}{4\,\frac{d\Gamma}{dc} + 3.5\,\frac{R_{Pb}^2}{R_b} + 3.5\,h_{cr}}$$

where R_{Pb} is the radius of curvature of the Plateau border P_b and R_b is the P_b length (in the order of the bubble radius). In most cases h_{cr} is negligible as is small compared to one of the other two terms.

Surfactant accumulation in the top layer and evaluation of the overall foam stability may be further complicated by droplet formation and spreading during rupture of the thin films. Droplet formation is an interesting phenomenon that can occur in various foam systems and is strongly influenced by the bubble dimensions and surfactant concentrations. It was first described by de Vries and explained as a capillary wave mechanism (Vrij, 1966b). With decreasing average film thickness h, the attractive disjoining pressure Π enhances the amplitude of some modes of thermally excited capillary waves present at film surfaces. At a given critical film thickness h_{cr}, corrugations on the two opposite film surfaces can touch each other resulting in the rupture of the thin film (Ivanov, 1980). The process of droplet formation and spreading will affect local surfactant concentrations though surfactant transport with the droplets.

4.1.2. Solid-stabilized foams

Many similarities can be observed in the behaviour of small solid particles and surfactant molecules at L-L and G-L interfaces. Important differences also exist. Stability of emulsions stabilized by solid particles is well studied and presented in the next chapter (4.2.7). Influence of the solid particles on the formation and stability of the foams is highly dependent on the surfactant type, particle size and their concentration (Kruglyakov and Taube, 1972; Pugh, 1996). Hydrophilic particles are known to enhance foam stability as they accumulate in the Plateau borders and slow down film drainage. Hydrophobic particles, on the other hand, enter the L-G interfaces of the foam and contribute to destabilization via the so-called bridging-dewetting mechanism (Garrett, 1980). The mechanism implies that a solid particle comes in contact with two opposite surfaces of the foam film and forms a solid bridge between them. Then, the particle is dewetted by the liquid and the three phase contact lines come in direct contact as the thin interfacial film gets perforated at the particle surface.

4.2. Emulsions

The theoretical results and experimental data discussed in section 3 refer to a single droplet or the limiting case of dilute emulsion where overall system dynamics and interactions can be neglected. Several specific cases are discussed below.

4.2.1. Emulsion separation in gravity settlers or separators

A mathematical model taking into account the droplet size distribution and using rate expressions for the description of droplet-droplet and droplet-interface coalescence was developed for prediction of emulsion separation in horizontal gravity settlers (Padilla et al., 1996). Experimental data was obtained in a continuous laboratory mixer-settler to verify the model. It was registered that the dispersion band thickness (layer between separated phases) decreased as the droplet size increased. The band thickness was also more sensitive to the inlet droplet size in the large size range. The obtained expression for the droplet-droplet coalescence frequency described well droplet growth rate from the passive to the active interface.

$$\lambda\,(v, v', z) = \lambda_o\,z\,\left(v^{-\frac{1}{3}} + v'^{-\frac{1}{3}}\right)^2$$

Where $\lambda_o = 0.13 \times 10^{-4} cm/s$ for the used emulsion system (10% Acorga M5640 in Escaid 103–0.25 M Na_2SO_4 aqueous solution), z is the height above the passive interface and at an arbitrary distance from the settler inlet and v is the volume of droplets in the band characterizing their size. The droplet-interface coalescence frequency was found to be independent of the droplet size and the thickness of the dispersion band; that is $\lambda^*(v, H) = \lambda_o^*$ $(\lambda_o^* = 0.305\ s^{-1})$ for the considered emulsion system.

The effect of turbulence on the separation of W/O and O/W emulsions in batch settlers was predicted by a model describing emulsion height H_o and holdup ε_o with an initial droplet diameter φ_o and interfacial coalescence time τ_d allowing for the turbulence decay time t_d and coalescence incubation time t_o (Fig. 8) (Jeelani et al., 1999). Batch separation of W/O and O/W emulsions sampled directly from a process stream or formed in a mixer are schematically illustrated in Figure and Figure. As residual turbulence is present in both cases, the separation is partly hindered by it. The turbulence also delays the interfacial coalescence until a time t_o. For a given batch emulsion, the sedimentation and coalescence profiles for different interfaces could be predicted by knowing the values of the initial sedimentation velocity of the droplets v_o, the maximum interfacial coalescence rate ψ_m, the time taken for the decay of turbulence t_d, and the incubation time for interfacial coalescence to begin t_o..

Many of the existing models apply to specific separator geometries at steady-state conditions. The original model used in the next study was developed for the steady-state operation of a settler with a wedge-shaped emulsion band (Ruiz, 1985). A modification of that numerical model was later applied for computing thickness and droplet-size composition of an emulsion band formed in a shallow-layer settler under dynamic conditions (Gomes et al., 2007). Separation predictions were confirmed to be satisfactory for small step-changes (wedge of the emulsion band compared every 10 cm) and were in close agreement with the experimental data.

A modification of Hartland's models for emulsion phase separation was used in combination with settling experiments performed on a dispersion rig set up. The new model included only one fitting parameter, namely droplet collision efficiency (α), which is characteristic for each specific emulsion system and is a function of the interfacial film elasticity and rate of the film drainage (Noïk et al., 2013). One of the main assumptions of the new model is based on using the initial droplet

[7] HLB values of a selection of surfactants correlated against use (Griffin, 1949).

[8] The HLB determines whether a surfactant is hydrophilic or lipophilic.

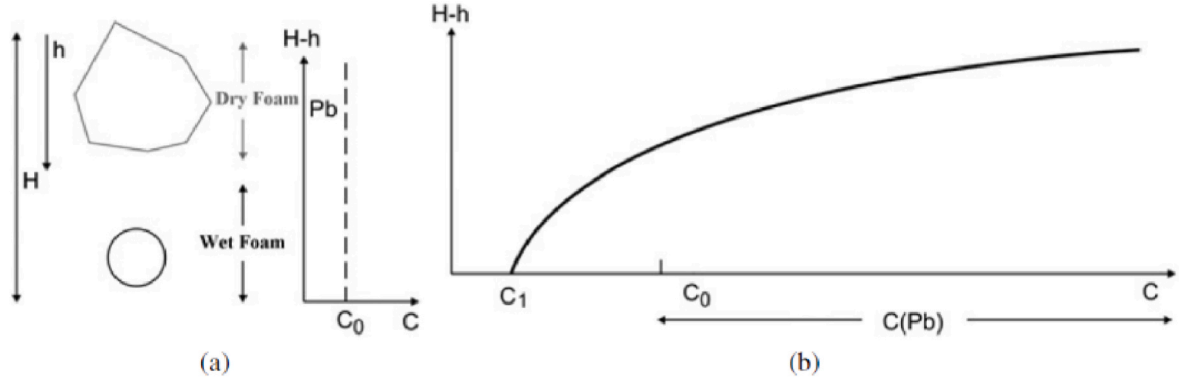

Fig. 6. Models for surfactant distribution within dry foam. a) Uniform surfactant distribution, (b) increasing surfactant concentration with decreasing distance (h) from the foam top (H is the foam height) (Dukhin et al., 2008).

volume as a basis for prediction of the droplet volume evolution, which also explains model's sensitivity to the variations in droplet sizes.

$$\frac{1}{\nu_o}\frac{d\nu}{dt}=\alpha\frac{1}{\tau_c}$$

where ν is the droplet volume evolution, ν_o is the initial droplet volume, $\frac{1}{\tau_c}$ is the parameter representing the mean collision frequency between droplets of diameter D with the characteristic collision time τ_c. D is the average droplet diameter in volume (D50, ν) of the droplet population.

A comprehensive model for prediction of settling behaviour of W/O emulsions was recently developed by Li et al. (2021). The model included water fraction and viscosity predictions, droplet displacement calculations, and droplet breakdown probability factor, the latter allowing for adjustment of the modelling predictions towards specific emulsion systems. Gravitational emulsion separation model formulated as a population balance equation was presented by García et al. (2022). A modification of Kynch's theory, typically used to predict solid particle sedimentation, was implemented. The model successfully predicted continues emulsion separation and droplet coalescence and was found to be more accurate compared to an earlier model developed by the authors (García and Betancourt, 2019).

4.2.2. Dense-packed layer

As illustrated in Figure and Figure, a DPL is expected to be present in separating emulsion systems. Formation and methods for DPL prediction have extensively been studied by Hartland and colleagues, who also established the following equation for the change of the DPL droplet diameter (Hartland and Jeelani, 1988):

$$\frac{d\,(d_{32})}{dx}=\frac{d_{32}}{6\,\tau_d u_m}$$

where τ_d characterises the droplet-droplet coalescence time. The same group developed a model for prediction of DPL/emulsion separation profiles taking into account the initial droplet diameter and interfacial coalescence times for an emulsion of given height, dispersed phase holdup, and physical properties (Fig. 7) (Jeelani and Hartland, 1998) of the most recent publications predicts the initial thickness of the DPL as a function of surfactant (Span 80) concentration and mean droplet size (Dinh et al., 2020). It is assumed that the coalescence rate only depends on the area of the thin film between two droplets. The quantitative model for the DPL separation kinetics allows for estimation of the coalescence frequency per unit area, which can be verified by simple bottle test experiments. A complete time evolution of the DPL separation kinetics is described by the following equation:

$$\frac{d\,L}{d\,t}=-\frac{A\,L}{\tau_c}\left(1-\frac{L}{L_o}\frac{t}{\tau_c}\right)^{-4/3}$$

where L is the DPL thickness, L_o is the initial DPL thickness, τ_c is the characteristic time describing a quasi-plateau and $A=\frac{R_o}{3\,L_o}$ (R_o is the mean droplet radius).

4.2.3. Modelling of phase inversion

Phase inversion or a shift from an O/W to a W/O emulsion and vice versa may occur at a range of water fractions. This behaviour can critically influence emulsion viscosity and pressure drop, which is unfavourable in pipes and boosting systems. Predicting phase inversion is therefore important and may be based on minimising the free energy of the system, which can be considered equal to the interfacial energy (Brauner, 2003). The interfacial energy is directly related to the droplet size and concentration, which have to be known or predicted beforehand. Brauner and Ullmann combined a methodology to predict the droplet size during pipe flow and used it as a closure for a model predicting the phase inversion point in dilute and highly viscous emulsion systems (Brauner and Ullmann, 2002). Being reliable for unstable systems, these models might fail in the presence of surfactants. As demonstrated by Plasencia (2013) after addition of surfactant the inversion point of a model oil-water system changed from 40% to 80% WC. Indeed, many crude oil systems show phase inversion at rather high water cuts (>50%) independent of the oil viscosity.

4.2.4. Concentrated emulsions

Concentrated emulsions are defined according to the volume fraction of the dispersed phase being greater than 12–20 vol % (Tadros, 2013b).

4.2.4.1. Laminar flow. One of the cases of interest arises from the flow of crude oil emulsions at low velocities in horizontal pipes. Coalescence plays a dominant role at low Re numbers, and emulsion destabilization can occur leading to formation of a second continuous fluid layer. This will in turn affect the effective viscosity of the mixture, which affects pressure drop inside the pipeline. One of the most interesting and industrially relevant cases is concentrated emulsions. The Ca^* values here are found to be below the lowest limit and are strongly concentration dependent. A generalization can still be applied by modifying the definitions for Ca^* and λ and substituting viscosity of the continuous phase η_o by the emulsion viscosity η_{em}. The expression for the modified "mean field" Ca_m given by (Jansen et al., 2001):

$$Ca_m=\frac{\eta_{em}\,\dot{\gamma}}{\sigma/R}$$

where $\dot{\gamma}$ is the shear rate, σ is the interfacial tension, and R is the droplet radius. The corresponding modified viscosity ratio λ_m can be expressed as:

$$\lambda_m=\eta_{dr}/\eta_{em}$$

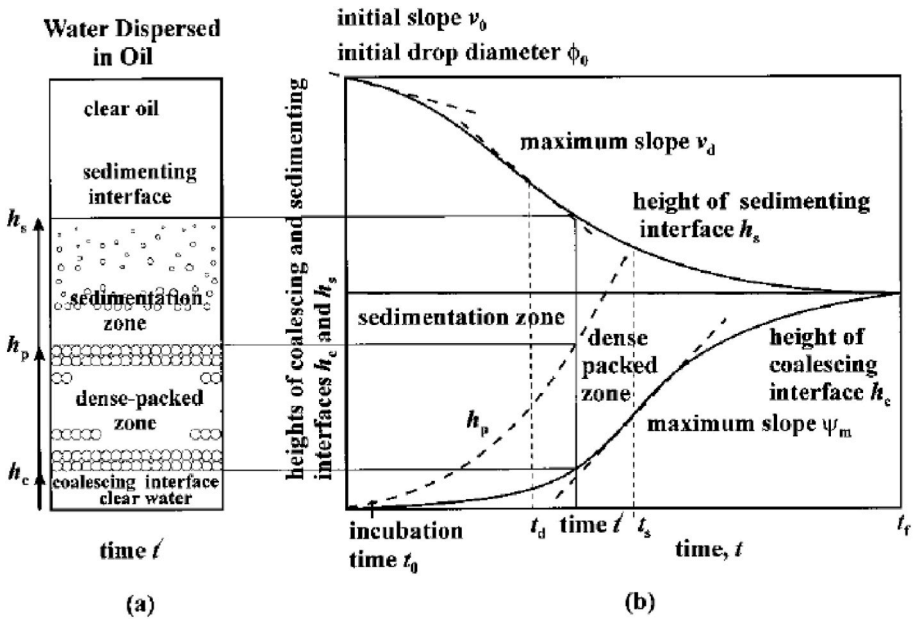

Fig. 7. Schematic diagram showing the heights of the sedimenting (upper) and coalescing (lower) interfaces in W/O emulsion. (b) Variation with time in the heights of the sedimenting (upper) and coalescing (lower) interfaces in W/O emulsion (Jeelani et al., 1999).

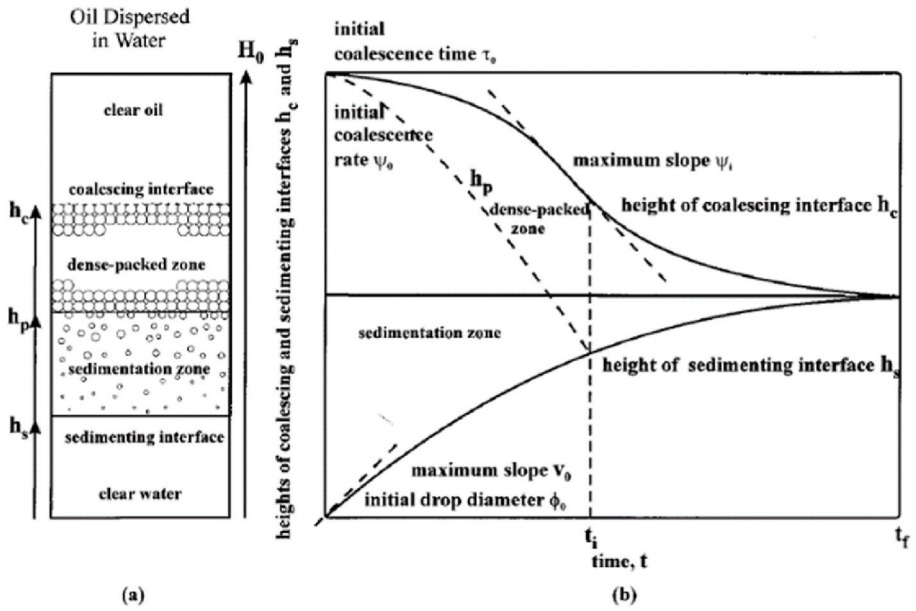

Fig. 8. Heights of the sedimenting and coalescing interfaces and the DPL formed at the top of a O/W emulsion due to the upward sedimentation of lighter oil drops in heavier water. (b) Schematic variation in the heights of sedimenting and coalescing interfaces in O/W emulsion (Jeelani and Hartland, 1998).

Where η_{dr} is the viscosity of the dispersed phase (droplet). The effect of droplet concentration is also shown in Fig. 9, where the critical shear rate ($\dot{\gamma}^*$) for the condition of breakup is presented as a function of the reciprocal droplet radius for emulsions of different concentrations (laminar flow conditions). As the concentration increases, the lower is the shear rate required for the droplet breakup to occur. Obtained

The droplet breakup at a given shear rate can continue up to a limiting droplet size (R_{lim}). R_{lim} s dependence on the shear rate ($\dot{\gamma}^*$) is described by a parabolic law. The following scaling law then becomes valid (Mason and Bibette, 1996):

$$R_{lim} = C\,\frac{\sigma}{\eta\,\dot{\gamma}}$$

where C is the factor in order of 1 (reflecting the critical capillary number Ca^*).

4.2.4.2. Turbulent flow. The transition to higher velocities and corresponding transition to turbulent flow significantly complicates prediction of the droplet breakup. Large fluctuations of local velocities and stresses inherent to turbulent flows make it difficult to experimentally confirm numerical results. This has been illustrated by Sleicher already in 1962 (Sleicher, 1962). "Inertial turbulent" (TI) and "viscous turbulent" (TV) flow regimes are generally accepted as two different modes of turbulent flows, which differ in the ratio of characteristic sizes of a liquid droplet and a turbulent vortex (Kolmogorov, 1949; Hinze, 1955). The minimal droplet size in the TI regime depends on the ratio of dynamic pressure fluctuations (breakup of a droplet) and surface tension. Droplet

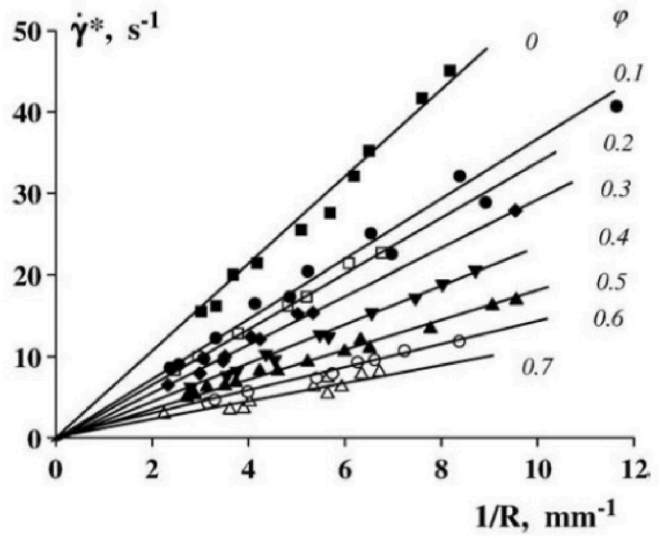

Fig. 9. Dependence of the critical shear rate vs. droplet breakup on droplet size in emulsions of different concentrations (Jansen et al., 2001).

breakup in the TV regime occurs under shear stresses acting via the continuous phase. For low viscosity droplets, the following equations of the maximum stable droplet size are valid for TI and TV regimes, respectively (Vankova et al., 2007):

$$D_{TI,max} = A_1\left(\varepsilon^{-2/5}\,\sigma^{3/5}\,\rho_c^{-3/5}\right) = A_1 d_k$$

where A_1 is the front-factor of the order of 1, ε is the intensity of energy dissipation, and ρ_c is the continuous phase density. The term in brackets designated as d_k is a characteristic length.

$$D_{TV,max} = A_2\left(\varepsilon^{-1/2}\,\eta_c^{-1/2}\,\rho_c^{-1/2}\,\sigma\right)$$

where the constant $A_2 \approx 4$ and η_c is the viscosity of the continuous phase.

For emulsions with arbitrary viscosity of phases, a generalization can be applied, resulting in the following formula for the maximum stable droplet size (Eastwood et al., 2004):

$$D_{TV,max} = A_3\left(1 + A_4\frac{\eta_{dr}\,\varepsilon^{1/3}\,D_{TV,max}^{1/3}}{\sigma}\right)^{3/5} d_k$$

where A_3 and A_4 are the constants, η_{dr} is the viscosity of the dispersed droplets.

An important factor in "natural" (production) formation of crude oil emulsions is contribution of turbulence or mixing. At the same time, emulsion separation or coalescence is affected by the turbulence energy (Schubert and Armbruster, 1992b).

4.2.5. Dilute emulsions in turbulent flows

Experiments investigating the influence of dispersed-phase viscosity and interfacial tension on the Sauter mean diameter (d_{32}) were performed in a stirred tank by Wang and Calabrese (1986). Droplet sizes for low to moderate viscosity dispersed phases were found to be normally distributed in volume and could be correlated by normalization with d_{32}. The final correlation of d_{32}/L was as follows:

$$\frac{d_{32}}{L} = 0.053\,We^{-3/5}\left[1 + 0.97Vi^{0.79}\right]^{3/5}$$

where L is the impeller diameter, Vi is the "tank viscosity group" or capillary number representing the ratio of dispersed phase viscous to surface forces, We is the tank Weber number. It was shown that the droplet size distributions broadened as the interfacial tension and viscosity increased and as impeller speed decreased. At constant emulsification conditions, the relative influence of interfacial tension decreased as the dispersed phase viscosity increased. For low interfacial tension systems, surface resistance to breakage become negligible relative to viscous resistance.

4.2.6. Fine emulsions

If droplets are sufficiently small (micrometre scale or smaller), it is the Brownian motion and not sedimentation that defines the coagulation behaviour of an emulsion. For microemulsions, droplet surface deformation is typically small and can be considered as negligible (solitary and well-separated droplets). However, in the case of highly concentrated emulsions, droplet deformation can play a significant role in the efficiency of coalescence process and overall emulsion separation, as the coalescence efficiency of slightly deformable droplets results from an interplay between the thin film resistance and short-range molecular attractions.

4.2.7. Particle stabilized emulsions

Emulsions stabilized by highly dispersed solid particles assembled at the interfaces are known as Pickering emulsions (Pickering, 1907). Examples of how spherical particles can adsorb at the water-air or water-oil interfaces are shown in Fig. 10 (lower left corner - solid-stabilized aqueous foams or O/W emulsions, lower right corner - solid-stabilized aerosols or W/O emulsions may form) (Binks, 2002). The relevant parameter is contact angle (θ), which the particle makes with the interface as particle wettability plays the major role. Emulsion viscosity in Pickering emulsions will increase with particle concentration, and the stabilization is dependent on the particle shape, size, concentration, wettability, and ability to interact with the interfaces (Sacanna et al., 2007). In reality, the stability and rheology of the Pickering emulsions are determined by the interactions between the solid particles and low molecular weight surfactants. Stabilization is only possible if the particles are smaller than emulsion droplets. Nano-meter scale particles form a solid-like network typical for "mild" elastic bodies. Even a small decrease in size (from 20 to 10 nm) may lead to a significant change in the rheology of the system. The elastic modulus of a system containing 10 nm particles is independent on frequency, which is characteristic for elastic materials. At the same time, particles with sizes less than 0.5 nm are governed by Brownian motion and do not accumulate at the interfaces (no contribution to emulsion stability) (Binks, 2002). Thus, there is a clear similarity in the behaviour of structured systems stabilized by solid particles and highly concentrated emulsions.

In cases when use of surfactants shall be avoided due to environmental concerns, use of particles may be an efficient option for emulsion formation and stabilization. A first order theoretical model for the case of O/W emulsion formation in presence of particles was recently developed by Stern et al. (2022). Interfacial energies, component densities, particle sizes and the agitation rates were included as

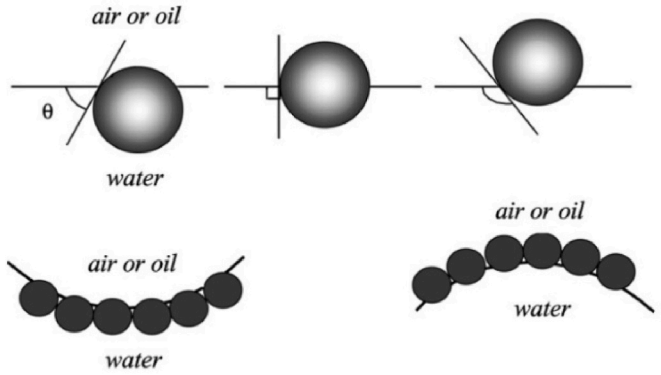

Fig. 10. Adsorption of spherical particles to different interfaces (Binks, 2002).

Table 1
HLB range and surfactant use.

HLB range	Use
1 to 3	Anti-foaming agent[8]
3 to 6	W/O emulsifier
7 to 9	Wetting agent[8]
13 to 16	Detergent[8]
8 to 16	O/W emulsifier
16 to 18	Solubiliser or hydrotrope[8]

emulsion-specific parameters. The model was successfully able to predict the rate droplet formation in studied Pickering emulsion systems. A combined effect of particles and surfactants on emulsion stability was modelled by Ali et al. (Ali and Chakrabarti, 2022). The two machine learning algorithms developed in this study were able to predict emulsion stability with 45–60% accuracy. The model, however, correctly indicated that higher water solubility of surfactants and extended mixing result in higher emulsion stability.

It is important to mention that surfactants added or present in emulsion systems containing solid particles will modify the particle wettability and can therefore reduce or enhance emulsion stability. One concrete example is a study describing the effect of Span 80 surfactant on the hydrophobicity of layered double hydroxide (LDH) (prone to stabilizing O/W emulsions). Water-in-paraffin oil emulsions were stabilized by the mixture of Span 80 and LDH, resulting from hydrophilization of the particles (Wang et al., 2009). Certain surfactants, including Span 80 may, at concentrations above the critical micelle concentration, also fully displace particles from the interfaces and contribute to reduced emulsion stability (Drelich et al., 2010).

4.2.8. Droplet coalescence in pipe flow

Pereyra et al. applied a mechanistic model for separation of O/W emulsions in a horizontal pipe settler by transforming the separation time of the batch settler to a residence time of the mixture in the pipe (Pereyra et al., 2013). The separation time was calculated by dividing the streamwise axial length of the pipe with the characteristic convective time of the flow. The model could predict droplet concentrations and thickness of the continuous layers in the vertical direction and along the pipe by simply considering two timescales characterising droplet-droplet and droplet-interface coalescence (Voulgaropoulos, 2017). The model assumes one average droplet size and, thus, neglects polydispersity of the emulsion system.

5. Modelling surfactant contribution

For surfactants present in oil/water systems, the HLB (hydrophile-lipophile balance)[9] value is often considered to be the most important parameter in determining whether the surfactant micelles or micro-emulsion droplets will reside in water, oil or a third phase. Generally, a HLB value below and above 10 indicate whether the surfactant is oil or water soluble respectively. Furthermore, HLB may be correlated against its behaviour as given in Table 1. The limitation here is that the HLB values were originally derived based on the data obtained at ambient temperature (Griffin, 1949). Models predicting surfactant effects on emulsion or foam stability generally assume reduction of surface tension as the main contribution from surfactants. It can be mentioned here that the temperature fluctuations and interactions with the aqueous and oil phases have to be taken into account as they may have just as significant effect on the surface tension as surfactant presence. The effect of the molecular characteristics of surfactants can be predicted based on the certain surfactant-specific parameters. For instance, an increase in the surfactant chain length is known to promote reduction of the surface tension at low surfactant concentrations (Smit et al., 1990). Ordering of the surfactant head groups normal to the interface may determine the effectiveness of the surfactants with branching of the hydrophobic tails (Rekvig et al., 2003). In some cases, addition of surfactants may also result in formation of equilibrium colloidal systems (surfactant levels exceeding CMC). The generic phase behaviour of non-ionic surfactants is illustrated in Fig. 11 (Davis, 1994).

The current chapter is limited to the molecular-based surfactants. However, it should be mentioned that emulsions can also be effectively stabilized by particle-based surfactants (Pickering stabilization is mentioned in 4.2.7). Non-ionic surfactants[10] are often used for stabilization of model/mineral oil emulsions and/or so-called reference fluids developed to investigate and predict dynamics of emulsion stability in real crude oil systems (Voulgaropoulos, 2017; Simonsen et al., 2014). One of the commonly used examples is Span 80, which is a sorbitan ester of a naturally occurring oleic acid. In agreement with its HLB value of 4.3, the surfactant is highly effective at forming O/W emulsions. Surface tension of a system stabilized by a non-ionic surfactant can be calculated by combining Gibbs adsorption equation for non-ionic surfactants with Langmuir adsorption isotherm. The final surface equation of state (EOS) can be written as:

$$\sigma = \sigma_o - \acute{R}\, t\, \Gamma_\infty \ln(1 + K_{Lc})$$

where σ_o is the surface tension of a system without surfactant, Γ_∞ is the adsorption capacity, K_L is the ratio between the adsorption and desorption rate constants, $\acute{R}$ is the universal gas constant, t is the temperature and c is the molar concentration of surfactant in the bulk. The EOS equation can be used to link concentration of a non-ionic surfactant to the interfacial tension of a system. Another way to predict not only the surface tension, but also the dynamic surface tension is by using statistical mechanical models incorporating surfactant tail length, concentration, and temperature (Cho et al., 2018).

5.1. Surfactant effect on the neck expansion velocity of bubbles and droplets

As mentioned in section 3.1, neck expansion velocity is a second defining factor in the rate of coalescence (after the thin film thinning). Results of numerical simulations reveal that the surfactant concentration along the interface of coalescing droplets and bubbles is not uniform during coalescence, and two peaks of concentration are located symmetrically on either side of the neck for the initial times (Martin and Blanchette, 2015). It was recently estimated that the presence of surfactants modifies the geometry of the approaching interfaces compared to systems without surfactants. The case of Span 80 dissolved in the bulk phase is presented by Chinaud et al. (2016). These models predict surfactant effect on partial coalescence of droplets and bubbles with a flat

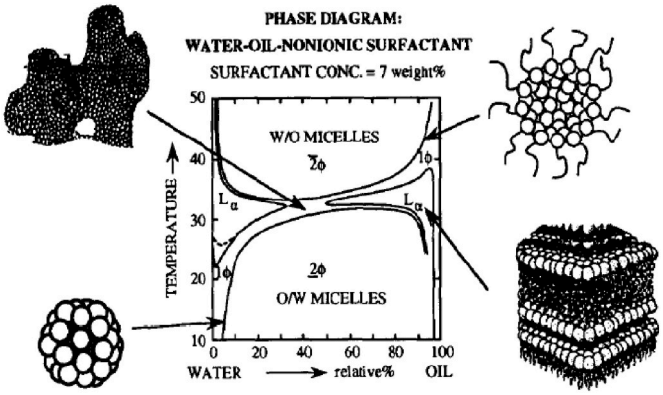

Fig. 11. *Phase diagram of $C_{12}E_5$, n-octane and water* (Davis, 1994).

[9] HLB of the non-ionic surfactants ranges from 0 to 20 (0–6 being hydrophobic, 6–9 water dispersible, and 9–20 hydrophilic).

fluid interface, however, similarities can be drawn towards droplet-droplet and bubble-bubble coalescence.

5.2. Surfactant effect on emulsion viscosity (rheology)

The correlation of surfactant concentration and type on the viscosity of polysaccharide emulsions (weak gel-like medium) was studied by Manca et al. (2001). Abil B8842 (high-molecular weight) and Triton N101 (low-molecular weight) surfactants were used. One can see that the concentration of both surfactants leads to viscosity reduction at low shear rates, which is followed by its significant increase at high shear rates (Manca et al., 2001). Opposite behaviour of the 40 wt% Triton N101 emulsions can be explained by the structural contribution of the surfactant molecules at this high concentration (no more details are given). It was suggested that at low shear rates, the polysaccharide matrix shows a limited connectivity induced by surfactant micelles (this associates with disruption in connectivity between the polymer chains). At high shear rates, smaller gel domains are formed and the surfactant contribution to the increase in system rheology is expected.

More sources refer to the mechanisms of surfactant contribution to emulsion viscosity. The increase in emulsion viscosity caused by the low-molecular weight surfactants leads to reduced mobility of the continuous phase due to formation of micelles at high surfactant concentrations (Reynolds et al., 2001). If high molecular weight surfactants are used, the increase in viscosity can be explained by the adsorption of large molecules and consequent formation of structured interfacial layers (example of protein-stabilized emulsions) (Dimitrova and Leal-Calderon, 2004).

5.3. Surfactant effect on foam stability

The effect of the non-ionic surfactants on the interactions in the thin foam films is typically estimated by the dependence of the equilibrium film thickness on the surfactant concentration. According to a range of studies summarized by Manev and Nguyen (2005), the equilibrium film thickness is also dependent on the pH and increases with increasing alkalinity, and the maximum equilibrium thickness (at a given ionic strength) has similar values for the majority of non-ionic surfactants. At the same time, the electrostatic disjoining pressure decreases at high surfactant concentrations, which directly affects formation of the equilibrium films. Experimental characterization of the foamability or foam stability of a solution can be performed using a number of techniques, including Bikerman's method, the Ross-Miles method, and the Bartsch method (Pugh, 2016). Prediction of the foamability of a surfactant solution seems to be difficult when the results are correlated to the bulk surfactant concentration. More clear correlations can, however, be established with regard to the surfactant type, surface tension and/or surface mobilities and surface elasticities calculated from the surface tension values (Petkova et al., 2020). An example showing the volume of entrapped air after 100 shakes (shaking method) in solutions stabilized by a range of ionic and non-ionic surfactants is given in Fig. 12. Significant differences in the foaming profiles of the non-ionic and ionic surfactants are observed. In the case of ionic surfactant, electrostatic repulsion between the foam film surfaces stabilizes the dynamic foam films already at moderate surface coverage and relatively high ionic strength (up to 100 mM NaCl). A dimensionless parameter 'foamability number' (Ω), which is a compilation of surfactant concentration, surface tension, surface concentration, molecular weight, and diffusion coefficient, was introduced to evaluate the surfactant contribution (Verma et al., 2020). It was shown that the Ω and solution foamability had a linear relationship for the tested solutions containing cationic and anionic surfactants.

Modelling and experimental efforts with emphasis on interfacial rheology and stress-deformation behaviour of interfaces containing different surfactant types have been summarized in a comprehensive review by Sagis (2011). The transient evolution of the flow around a

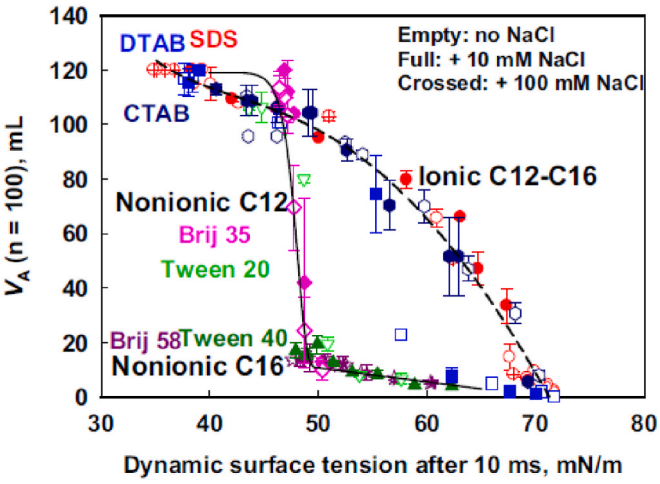

Fig. 12. Volume of trapped air vs. dynamic surface tension (Petkova et al., 2020).

spherical bubble rising in a liquid containing a partially soluble surfactant was numerically simulated by Cuenot and Jacques (1997). The model accounted for bulk mass surfactant transfer, adsorption and desorption parameters, which are often neglected in models. The results describe the temporal evolution of the relevant scalar and dynamic interfacial quantities as well as the changes in the flow structure and the increase of the drag coefficient. These effects are mostly relevant for bubbly flows. It has also been shown that mixing liquids of different polarities may result in a surfactant-like behaviour of the liquid with smaller surface tension (Tran et al., 2020). In this case, foam or froth formation is expected. Thin film thickness reached by the liquid films before drainage was computed from the experimental variations of surface tension with the mixture composition. The described effect is noted to have potentially large consequences for the flow of fluids in contact with gases. Among some of the recent attempts to model surfactant-dependent thin film drainage at L-L and L-G interfaces are the works by Ozan and Jakobsen (Ozan and Jakobsen, 2019, 2020; Ozan et al., 2021). Effects of surface rheology on the drainage of thin films containing low surfactant concentrations (inhomogeneous coverage) were investigated for the systems with water as continuous phase. Marangoni stresses and surface viscosities were shown to have a significant effect on the coalesce timescales of bubbles and droplets with viscosity similar to the one of water. The two parameters were, however, mentioned to overshadow each as simulation parameters were varied. Presence of surfactants were shown not only to contribute to the occurrence of Marangoni flows, but also to increase interface immobility through contribution to higher interfacial viscosity. Droplet and bubble approach velocity had a significant effect on the surface rheological parameters (Ozan and Jakobsen, 2019). A surface analogous of the Upper Convected Maxwell model was used to estimate the effects of surface viscoelasticity on the thin film drainage between two fluid droplets. The model was developed a surfactant-laden surface with uniform molecular distribution over the interface. Time dependent viscoelasticity was shown to be essential for accurate prediction of the coalesce timescales. This was associated with the behaviour shift resulting from elastic forces and interface mobility affected by surfactant presence (Ozan and Jakobsen, 2020).

5.4. Emulsions

Emulsion stability is determined mainly by the elasticity (thermodynamic factor) and viscosity (kinetic factor) in droplet interactions (Izmailova et al., 2000; Danov, 2001), both of which closely interrelate with the intermolecular interactions in surfactant layers adsorbed at the interfaces. The chemical nature of each specific surfactant and fluid

system represents the primary practical interest. Depending on the surfactant type, the two effects either have the same order of magnitude, or the surface elasticity is more important than the surface viscosity for the tangential mobility of interfaces and for its impact on the emulsion viscosity (Danov, 2001). When shear stress is applied, surfactants adsorbed at the interface will generate a stress gradient resulting in the increase of the elastic emulsion component (G′). This increase leads to consequent delay of droplet coalescence and increase in the overall emulsion stability. Interfacial adsorption layers of surfactants will, to a large degree, also influence viscosity and flow characteristics of emulsions under applied stress or force.

5.4.1. Dilute emulsions

Analysis of surfactant (presumed soluble in both phases) effects on the slow motion of a droplet in dilute emulsion system was performed by Danov (2001), who presented three key parameters influencing the flow of droplets: 1). The viscosity ratio of the phases, $\lambda = \eta_{dr}/\eta_o$; 2). The ratio of surface (2D) viscosity expressed as $\frac{\eta_{surf}}{\eta_o}$, and 3). Elasticity of the interfacial layer and diffusion of a surfactant expressed as $= \frac{Re_{Gs}}{2\eta_o D_{eff}}$, where Re_{Gs} is the surface elasticity modulus and D_{eff} is the apparent diffusion coefficient of the surfactant. If the droplet size distribution and the interfacial properties of the system are known, the effective viscosity of the emulsion can be calculated as:

$$\frac{\eta_r}{\eta_o} - 1 = \left(1 + \frac{3}{2}\langle\varepsilon\rangle\right)\varphi$$

where ε is the mobility parameter of the interfacial layer averaged for all droplets and depends on the three parameters listed above.

5.4.2. Concentrated emulsions

A model predicting influence of both the surfactant concentration and hydrodynamic conditions on the mean droplet diameter (d_{32}) was developed and experimentally confirmed using whey protein concentrate (as surfactant) (Tcholakova et al., 2003). The O/W emulsions were produced by passing through a homogenizer. The applied pressure at the inlet, flow rate, emulsification duration, and corresponding number of passes were varied. It was concluded that at low surfactant concentrations the Sauter mean droplet diameter d_{32} is governed by the surfactant specific threshold adsorption value (Γ*) and can be calculated as follows:

$$d_{32} \approx \frac{6\,\Phi\,\Gamma^*}{(1-\Phi)C_{PR}^{INI}}$$

where Φ is the volume fraction of the dispersed phase and C_{PR}^{INI} is the normalized surfactant concentration. The equation confirms that the d_{32} is independent of the dispersed phase volume fraction or the hydrodynamic regime. At high surfactant concentrations, however, d_{32} was found to be independent of the protein surfactant concentration and was determined mainly by the power of dissipation in the emulsification device.

The same model was later applied to evaluate the effect of surfactant type (anionic, non-ionic and protein), surfactant concentration and ionic strength of the aqueous solution (concentration of NaCl) in turbulent flow (Tcholakova et al., 2004). The model well described the defect of non-ionic and protein surfactant concentrations (low concentration range) on d_{32} at high NaCl concentration of 150 mM. The model was also found inapplicable to emulsions stabilized by the ionic and non-ionic surfactants at low NaCl concentrations.

5.5. Asphaltenes as crude oil emulsion stabilizers

Asphaltenes are known to form a cross-linked interfacial film responsible for the stability of crude oil emulsions. Just like surfactants, asphaltenes are assumed to follow a Langmuir type equation of state and their surface coverage is considered as to be the main contributor to the changes in interfacial tension (Interfacial Rheology of Asphaltenes at, 2013). As the interface becomes full of asphaltene molecules or their colloidal aggregates, and the critical surface coverages are reached, a subsequent reduction of the asphaltene surface mobility will cause resistance to droplet deformation and droplet coalescence. As resins are always present in crude oils, their contribution to the interface stabilization and interactions with asphaltenes have to be accounted for (2.2). Resins are structurally similar to asphaltenes, but smaller in molecular weight. This allows them to form “networks” with the asphaltene aggregates, which can diffuse and adsorb to the interfaces faster than pure asphaltene aggregates. At the interface, a molecular rearrangement occurs, and resins become the primary adsorbent by displacing the asphaltenes and possibly reducing the interface stability (Yang et al., 2007).

5.6. Role of production chemicals in crude oil emulsion stability

It is often observed that the stability of a crude oil emulsion can increase by up to 10-fold if certain production chemicals are leaked into or mixed with the fluid systems. Among other factors, the resulting stability increase arises from the decrease of the surface tension caused by the earlier discussed rearrangement and/or adsorption of additional surface-active compounds (both particulate and molecular-based). This effect is even more difficult to predict as the original surfactant concentrations, fluid temperatures, flow conditions and phase fractions are already dynamic parameters. The majority of the oil field production chemicals are water-soluble and may (under certain conditions) favour stable O/W emulsions (Hustad et al.). As the pH of the water phase affects emulsion stability, acidization operations must be properly designed. The expected changes in interfacial composition arising from surfactant concentration, surface activity, molecular dimensions, post-adsorption conformational changes, and interactions can be predicted through modelling (Guzmán et al., 2016). However, such models often require detailed knowledge about the molecular and physicochemical properties of the system. Without examples of the potentially introduced production chemicals, one could use mixed surfactant systems to better understand the combined effect of several stabilizers adsorbed at a L-L interface.

One relevant study investigated the effect of a range of chemicals on the properties of the interfacial films in model W/O toluene and heptane-toluene emulsions stabilized by asphaltenes as well as diluted water-in-bitumen emulsions (Ortiz et al., 2010). The investigated chemicals included Aerosol OT, nonyphenol ethoxylates, polypropylene oxide/polyethylene oxide block-copolymer, dodecylbenzene sulfonic acids (branched and linear), docecylbenzene sulfonic acid-polymer blend, diisopropyl naphthalene sulfonic acid, and sodium naphthenate. Emulsion stability was correlated to a stability parameter, which is a function of the crumpling film ratio and interfacial tension (or surface pressure). Either increase or decrease in emulsion stability was observed as a result of the surfactant addition. This mostly was attributed to their ability to eliminate the crumpling point. Surfactants that failed to do so consequently decreased the crumpling ratio (the surface area at which the film crumpled relative to the initial surface area).

6. Summary

The stability of emulsions and foams is considered to be a crucial component for modelling complex fluid systems such as crude oils and other surfactant-stabilized systems. Specifically, the stability of oil/water emulsions can have a substantial effect on the total pressure loss in oil production systems and may also have important implications with respect to the presence of free water and subsequent corrosion issues. Gas-liquid foaming may substantially affect the flow characteristics of systems, possibly leading to extremely long slugs that cause problems for the separation facilities.

This review highlights some of the key physical mechanisms that

govern droplet coalescence and break-up in the presence of surfactants, as well as various modelling efforts reported in the public literature. Many of the phenomena governing coalescence and break-up may be in practice impossible to model in detail because of the sheer complexity of the problem. Developing relatively pragmatic methods for modelling emulsion/foam stability, using simple characterization methods to calibrate the models for each specific fluid system, could be a promising approach. Still, a good understanding of the underlying fundamentals is important when formulating pragmatic models. Specifically, a general understanding of the most underlying phenomena will be helpful in establishing the limitations in the models, and to establish guidelines on how the models should be used. Some of the mechanisms to be considered in a model for emulsion/foam stability are.

1. Film drainage between colliding droplets, and the associated influence of surfactants.
2. Droplet collision frequency and efficiency.
3. Surfactant diffusion from the bulk to the interface.
4. Droplet deformation.

It should be noted that the studies reviewed in this document either consider liquid-liquid emulsions or gas-liquid foams, but none consider the simultaneous existence of both at the same time as may be the case in three-phase flows. Three-phase flows are common during production and transport in the oil and gas industry, and a relatively limited number of models exists for predicting three-phase flows (Zhang and Sarica, 2006; Cazarez et al., 2010), much less coalescence and separation in three-phase systems. It is thus unclear how emulsions and foams interact when simultaneously present in the same fluid bulk.

Declaration of competing interest

The authors declare that they have no known competing financial interests or personal relationships that could have appeared to influence the work reported in this paper.

Data availability

No data was used for the research described in the article.

Acknowledgement

The work was supported by the knowledge-building projects for industry “Nexflow” (NFR project number 295035) and “Enabling non-disruptive production conditions - slug flow with surfactants " (NFR Project number 280610) and the innovation project “ChemFlow” (NFR project number 314165). The authors acknowledge the Research Council of Norway and the industrial partners TotalEnergies EP Norge AS, Lundin Energy, ConocoPhillips for their financial support.

References

Ali, B.K., Chakrabarti, D.P., 2022. The impact of surfactants and particles on the stability of emulsion in the North Coast Marine Acreage of Trinidad and Tobago. J. Pet. Sci. Eng. 212, 110314.
Alvarez, N.J., Walker, L.M., Anna, S.L., 2010. A microtensiometer to probe the effect of radius of curvature on surfactant transport to a spherical interface. Langmuir 26 (16), 13310–13319.
Arbuzov, K.N., Grebenshchikov, B.N., 1937. On the study of foam stability. Zh. Fiz. Khim. 10, 32–39.
Ata, S., Pugh, R.J., Jameson, G.J., 2011. The influence of interfacial ageing and temperature on the coalescence of oil droplets in water. Colloids Surf., A 374, 96–101.
Auflem, I.H., 2002. Influence of Asphaltene Aggregation and Pressure on Crude Oil Emulsion Stability. NTNU, Trondheim.
Basheva, E.S., Gurkov, T.D., Ivanov, I.B., Bantchev, G.B., Campbell, B., Borwankar, R.P., 1999. Size dependence of the stability of emulsion drops pressed against a large interface. Langmuir 15, 6764–6769.
Berridge, S.A., Dean, R.A., Fallows, R.G., Fish, A., 1968. The properties of persistent oils at sea. J. Inst. Petrol. 54, 300–309.
Bhakta, A., Ruckenstein, E., 1995. Drainage of a standing foam. Langmuir 11 (5), 1486–1492.
Bhakta, A., Ruckenstein, E., 1997. Drainage and coalescence in standing foams. J. Colloid Interface Sci. 191 (1), 184–201.
Bikerman, J.J., 1953. Foams: Theory and Industrial Applications. Reinhold Publishing.
Binks, B.P., 2002. Particles as surfactants - similarities and differences. Curr. Opin. Colloid Interface Sci. 7, 21–41.
Borisevich, J.P., Krasnova, G.Z., 2010. Mechnism of intermeduaite emulsion layer formation in process equipement. In: IV International Scientic-Applied Conference on "Oil and Gas Technologies. Samara.
Brauner, N., 2001. The prediction of dispersed ows boundaries in liquid±liquidand gas ±liquid systems. Int. J. Multiphas. Flow 27, 885–910.
Brauner, N., 2003. Liquid-liquid two-phase flow systems. In: Modelling and Experimentation in Two-phase Flow. Springer, pp. 221–279.
Brauner, N., Ullmann, A., 2002. Modeling of phase inversion phenomenon in two-phase pipe flows. Int. J. Multiphas. Flow 28 (7), 1177–1204.
Cantat, I., 2018. Foams - Structure and Dynamics. Oxford University Press.
Cazarez, O., Montoya, D., Vital, A.G., Bannwart, A.C., 2010. Modeling of three-phase heavy oil–water–gas bubbly flow in upward vertical pipes. Int. J. Multiphas. Flow 36, 439–448.
Chinaud, M., Voulgaropoulos, V., Angeli, P., 2016. Surfactant effects on the coalescence of a drop in a Hele-Shaw cell. Phys. Rev. E 94, 033101.
Cho, H.J., Sresht, V., Wang, E.N., 2018. Predicting surface tensions of surfactant solutions from statistical mechanics. Langmuir 34, 2386–2395.
Christenson, H.K., Yaminsky, V.V., 1995. Solute effects in bubble coalescence. J. Phys. Chem. 99, 10420.
Clay, P.H., 1940. The mechanism of emulsion formation in turbulent flow. I. Proc. R. Neth. Acad. Arts Sci. 43, 852–865.
Cuenot, B., Jacques, M., 1997. The effects of slightly soluble surfactants on the flow around a spherical bubble. J. Fluid Mech. 339, 25–53.
Danov, K.D., 2001. On the viscosity of dilute emulsions. J. Colloid Interface Sci. 235, 144–149.
Danov, K.D., Vlahovska, P.M., Horozov, T., Dushkin, C.D., Kralchevsky, P.A., Mehreteab, A., Broze, G., 1996. Adsorption from micellar surfactant solutions: nonlinear theory and experiment. J. Colloid Interface Sci. 183, 223–235.
Davis, H.T., 1994. Factors determining emulsion type: hydrophile—lipophile balance and beyond. Colloids Surf., A 91 (3), 9–24.
Derjaguin, B.V., Churaev, N.V., Muller, V.M., 1987. He derjaguin—landau—verwey—overbeek (DLVO) theory of stability of lyophobic colloids. In: Surface Forces. Springer, Boston, MA, pp. 293–310.
Dimitrova, T.D., Leal-Calderon, F., 2004. Rheological properties of highly concentrated protein-stabilized emulsions. Adv. Colloid Interface Sci. 108, 49–61.
Dimitrova, B.S., Ivanov, I.B., Nakache, E., 1988. Mass transport effects on the stability of emulsion films with acetic acid and acetone diffusing across the interface. J. Dispersion Sci. Technol. 9, 321–341.
Dinh, H.-H.-Q., Santanach-Carreras, E., Schmitt, V., Lequeux, F., 2020. Coalescence in concentrated emulsions: theoretical predictions and comparison with experimental bottle test behaviour. Soft Matter 45.
Drelich, A., Gomez, D., Clausse, D., Pezron, I., 2010. Evolution of water-in-oil emulsions stabilized with solid particles: influence of added emulsifier. Colloids Surf., A 365, 171–177.
Dukhin, S.S., Kovalchuk, V.I., Aksenenko, E.V., Miller, R., 2001. Accumulation of surfactant in the top foam layer caused by ruptured foam films. In: Bubble and Drop Interfaces. CRC Press, London.
Dukhin, S.S., Kovalchuk, V.I., Aksenenko, E.V., Miller, R., 2008. Surfactant accumulation within the top foam layer due to rupture of external foam films. Adv. Colloid Interface Sci. 137 (1), 45–56.
Eastoe, J., Dalton, J.S., 2000. Dynamic surface tension and adsorption mechanisms of surfactants at the air–water interface. Adv. Colloid Interface Sci. 85 (2–3), 103–144.
Eastoe, J., Dalton, J.S., Rogueda, P.G., Griffiths, P.C., 1998. Evidence for Activation−Diffusion controlled dynamic surface tension with a nonionic surfactant. Langmuir 14 (5), 979–981.
Eastwood, C.D., Armi, L., Lasheras, J.C., 2004. The breakup of immiscible fluids in turbulent flows. J. Fluid Mech. 502, 309–333.
Exerowa, D.R., Kruglyakov, P.M., 1997. Foam and foam films: theory, experiment, application. In: Studies in Interface Science. Elsevier.
Fingas, M., Fieldhouse, B., 2003. Studiesoftheformationprocessofwater-in-oil emulsions. Mar. Pollut. Bull. 47 (9–12), 369–396.
García, A., Betancourt, F., 2019. Conservative mathematical model and numerical simulation of batch gravity settling with coalescence of liquid-liquid dispersions. Chem. Eng. Sci. 207, 1214–1229.
García, A., Berres, S., Mas-Hernández, E., 2022. A new mathematical model of continuous gravitational separation with coalescence of liquid-liquid emulsions. Chem. Eng. Res. Des. 182, 37–50.
Garrett, P.R., 1980. Preliminary consideration concerning the stability of a liquid heterogeneity in a plane-parallel liquid film. J. Colloid Interface Sci. 76, 587–590.
Gomes, E.F., Guimarães, M.M., Ribeiro, L.M., 2007. Numerical modelling of a gravity settler in dynamic conditions. Adv. Eng. Software 38, 810–817.
Grace, H.P., 1982. Dispersion phenomena in high viscosity immiscible fluid systems and application of static mixers as dispersion sdevices in such systems. Chem. Eng. Commun. 14, 225–277.
Grassia, P., Neethling, S.J., Cervantes, C., Lee, H.T., 2006. The growth, drainage and bursting of foams. Colloids Surf., A 274 (1–3), 110–124.
Griffin, W.C., 1949. Classification of surface-active agents by 'HLB. J. Soc. Cosmet. Chem. 1 (5), 311–326.

Guzmán, E., Llamas, S., Maestro, A., Fernández-Peña, L., Akanno, A., Miller, R., Ortega, F., Rubio, R.G., 2016. Polymer–surfactant systems in bulk and at fluid interfaces. Adv. Colloid Interface Sci. 233, 38–64.
Hartland, S., 1979. The effect of gravity on the drainage of thin films in two-dimensional dense-packed dispersions. Chem. Eng. Sci. 34 (4), 485–491.
Hartland, S., Jeelani, A.A., 1988. Prediction of sedimentation and coalescence profiles in a decaying batch dispersion. Chem. Eng. Sci. 43 (9), 2421–2429.
Henschke, M., Schlieper, L.H., Pfennig, A., 2002. Determination of a coalescence parameter from batch-settling experiments. Chem. Eng. J. 85 (2), 369–378.
Hinch, E.J., Acrivos, A., 1979. Steady long slender droplets in two-dimensional straining motion. J. Fluid Mech. 91, 401–414.
Hinze, O.J., 1948. Forced deformations of viscous liquid globules. Appl. Sci. Res. A1, 263.
Hinze, O.J., 1955. Fundamentals of the hydrodynamic mechanism of splitting in dispersion processes. AIChE J. 1 (3), 289–295.
B. M. Hustad, A.-M. Hårvik, A. M. Halvorsen and J. Waage, "Qualification of Production Chemicals - Challenges," Statoil.
Ivanov, I.B., 1980. Effect of surface mobility on the dynamic behavior of thin liquid films. Pure Appl. Chem. 52 (5), 1241–1262.
Ivanov, I.B., Kralchevsky, P.A., 1997. Stability of emulsions under equilibrium and dynamic conditions. Colloids Surf., A 128, 155–175.
Ivanov, I.B., Traykov, T.T., 1976. Hydrodynamics of thin liquid films. Rate of thinning of emulsion films from pure liquids. Int. J. Multiphas. Flow 2 (4), 397–410.
Ivanov, I.B., Danov, K.D., Kralchevsky, P.A., 1999. Flocculation and coalescence of micron-size emulsion droplets. Colloids Surf., A 152, 161–182.
Izmailova, V.N., Derkach, S.R., Levachev, S.M., Tampol'skaya, G.P., Tulovskaya, Z.D., Tarasevich, V.N., 2000. Properties of interfacial layers in multicomponent systems containing gelatin. Colloid J. 62, 653–675.
Jackson, N.E., Tucker, C.L., 2003. A model for large deformation of an ellipsoidal droplet with interfacial tension. J. Rheol. 47, 659.
Jansen, K.M., Agterof, W.G., Mellema, J., 2001. Droplet breakup in concentrated emulsions. J. Rheol. 45 (1), 227–236.
Jeelani, S.A., Hartland, S., 1998. Effect of dispersion properties on the separation of batch liquid-liquid dispersions. Ind. Eng. Chem. Res. 37, 547–554.
Jeelani, S.A., Panoussopoulos, K., Hartland, S., 1999. Effect of turbulence on the separation of liquid-liquid dispersions in batch settlers of different geometries. Ind. Eng. Chem. Res. 38, 493–501.
Karpenko, I.N., Konovalov, N.N., 2019. Investigation of Demulsifier Performance in Presence of HCl Acid. Samara State Technical University, Samara, Russia.
Kolmogorov, A.N., 1949. Desintegration of drops in a turbulent flow. Reports of the USSR Academy of Sciences 46, 945–964.
Kruglyakov, P.M., Taube, P.R., 1972. Syneresis and stability of foams containing a solid phase. Colloid J. 34.
Li, Y.-B., He, T.-S., Hu, Z.-M., Zhang, Y.-Q., Luo, Q., Pu, W.-F., Zhao, J.-Z., 2021. Study on the mathematical model for predicting settling of water-in-oil emulsion. J. Pet. Sci. Eng. 206, 109070.
Liu, J., Messow, U., 2000. Diffusion-controlled adsorption kinetics at the air/solution interface. Colloid Polym. Sci. 278, 124–129.
Liu, J., Wang, C., Messow, U., 2004. Adsorption kinetics at air/solution interface studied by maximum bubble pressure method. Colloid Polym. Sci. 283, 139–144.
Manca, S., Lapasin, R., Partal, P., Gallegos, C., 2001. Influence of surfactant addition on the rheological properties of aqueous Welan matrices. Rheol. Acta 40, 128–134.
Manev, E.D., Nguyen, A.V., 2005. Effects of surfactant adsorption and surface forces on thinning and rupture of foam liquid films. Int. J. Miner. Process. 77, 1–45.
Martin, D.W., Blanchette, F., 2015. Simulations of surfactant effects on the dynamics of coalescing drops and bubbles. Phys. Fluids 27, 012103.
Mason, T.G., Bibette, J., 1996. Emulsification in viscoelastic media. Phys. Rev. Lett. 77, 3481.
Megias-Alguacil, D., Windhab, E.J., 2006. Viscosity of a Newtonian fluid calculated from the deformation of droplets covered with a surfactant under a linear shear flow. Reol Acta 46 (2), 223–229.
Miller, R., Liggieri, L., 2011. Chapter 15," in Bubble and Drop Interfaces, pp. 385–400. Leiden, Boston.
Milton, J.R., Kunjappu, J.T., 2012. Surfactants and Interfacial Phenomena. Wiley.
Neethling, S.J., Lee, H.T., Grassia, P., 2005. The growth, drainage and breakdown of foams. Colloids Surf., A 263, 184–196.
Nguyen, A., Schulze, H.J., 2003. Colloidal Science of Flotation. CRC Press, Boca Raton.
Noïk, C., Palermo, T., Dalmazzone, C., 2013. Modeling of liquid/liquid phase separation: application to petroleum emulsions. J. Dispersion Sci. Technol. 34, 1029–1042.
Ortiz, D.P., Baydak, E.N., Yarranton, H.W., 2010. Effect of surfactants on interfacial films and stability of water-in-oil emulsions stabilized by asphaltenes. J. Colloid Interface Sci. 351, 542–555.
Ozan, S.C., Jakobsen, H.A., 2019. On the role of the surface rheology in film drainage between fluid particles. Int. J. Multiphas. Flow 120, 103103.
Ozan, S.C., Jakobsen, H.A., 2020. Effect of surface viscoelasticity on the film drainage and the interfacial mobility. Int. J. Multiphas. Flow 130, 103377.
Ozan, S.C., Hosen, H.F., Jakobsen, H.J., 2021. On the prediction of coalescence and rebound of fluid particles: a film drainage study. Int. J. Multiphas. Flow 135, 103521.
Padilla, R., Ruiz, M.C., Trujillo, W., 1996. Separation of liquid-liquid dispersions in a deep-layer gravity settler: Part I. Experimental study of the separation process. Hydrometallurgy 42 (2), 267–279.
Pereyra, E., Mohan, R.S., Shoham, O., 2013. A Simplified Mechanistic Model for an Oil/Water Horizontal Pipe Separator. Society of Petroleum Engineers. https://doi.org/10.2118/163077-PA.
Petkova, B., Tcholakova, S., Chenkova, M., Golemanov, K., Denkov, N., Thorley, D., Stoyanov, S., 2020. Foamability of aqueous solutions: role of surfactant type and concentration. Adv. Colloid Interface Sci. 276, 102084.
Pickering, S.U., 1907. CXCVI.—Emulsions," J Chem Soc 91, 2001.
Plasencia, J., 2013. Experimental study on two phase oil-water dispersed flow. In: Department of Energy and Process Engineering. Norwegian University of Science and Technology: Trondheim.
Poptoshev, E., Claesson, P.M., 2002. Role of hydration and conformational changes in adsorption dynamics of ethyl(hydroxyethyl)cellulose at the air/solution interface. Langmuir 18 (7), 2590–2594.
Pugh, R.J., 1996. Foaming, foam films, antifoaming and defoaming. Adv. Colloid Interface Sci. 64, 67–142.
Pugh, R.J., 2016. 11 - bubble size measurements and foam test methods. In: Bubble and Foam Chemistry. Cambridge University Press, Cambridge, pp. 372–404.
Radoëv, B.P., Dimitrov, D.S., Ivanov, I.B., 1974. Hydrodynamics of thin liquid films effect of the surfactant on the rate of thinning. Colloid Polym. Sci. 252, 50–55.
Radoev, B.P., Scheludko, A.D., Manev, E.D., 1983. Critical thickness of thin liquid films: theory and experiment. J. Colloid Interface Sci. 95 (1), 254–265.
Ravera, F., Liggieri, L., Steinchen, A., 1993. Sorption kinetics considered as a renormalized diffusion process. J. Colloid Interface Sci. 156 (1), 109–116.
Rekvig, L., Kranenburg, M., Havskjold, B., Smit, B., 2003. Effect of surfactant structure on interfacial properties. Europhys. Lett. 63 (6), 902–907.
Renardy, Y., 2007a. The effects of confinement and inertia on the production of droplets. Rheol. Acta 46 (4), 521–529.
Renardy, Y., 2007b. Drop oscillations under simple shear in a highly viscoelastic matrix. Rheol. Acta 47, 89–96.
Reynolds, P.A., Gilbert, E.P., White, G.W., 2001. High internal phase water-in-oil emulsions and related microemulsions studied by small angle neutron scattering. 2. The distribution of surfactant. J. Phys. Chem. B 105, 6925–6932.
Ruckenstein, E., Bhakta, A., 1996. Effect of surfactant and salt concentrations on the drainage and collapse of foams involving ionic surfactants. Langmuir 12 (17), 4134–4144.
Ruiz, M.C., 1985. Mathematical Modelling of a Gravity Settler," PhD Thesis. University of Utah.
Sacanna, S., Kegel, W.K., Philipse, A.P., 2007. Thermodynamically stable pickering emulsions. Phys. Rev. Lett. 98, 158301.
Sagis, L., 2011. Dynamic properties of interfaces in soft matter: experiments and theory. Rev. Mod. Phys. 83 (4), 1367–1403.
Sanfeld, A., Steinchen, A., 2008. Emulsions stability, from dilute to dense emulsions - role of drops deformation. Adv. Colloid Interface Sci. 140, 1–65.
Scheludko, A., 1962. Proc. Kon. Nederl. Acad. Wet. B 65, 76.
Schramm, L.L., 2005. Emulsions, Foams, and Suspensions: Fundamentals and Applications. WILEY-VCH Verlag GmbH & Co. KGaA, Weinheim, Germany.
Schubert, H., Armbruster, H., 1992a. Principles of formation and stability of emulsions. Int. Chem. Eng. 32, 14–28.
Schubert, H., Armbruster, H., 1992b. Principles of formation and stability of emulsions. Int. Chem. Eng. 32 (1), 14–28.
Sheludko, A., 1967. Thin liquid films. Adv. Colloid Interface Sci. 1, 391–464.
Simonsen, G., Pettersen, B., Kelesoğlu, S., Sjöblom, J., 2014. Preparation and characterization of reference fluid mimicking behavior of North Sea heavy crude oil. Fuel 135, 308–314.
Sleicher, C.A., 1962. Maximum stable drop size in turbulent flow. A.l.Ch.E. Journal 8 (4), 471–477.
Smit, B., Schlijper, A.G., Rupert, L.A., Van Os, N.M., 1990. Effects of chain length of surfactants on the interfacial tension: molecular dynamics simulations and experiments. J. Phys. Chem. 94 (18), 6933–6935.
Stern, Y., Tadmor, R., Multanen, V., Oren, G., 2022. A first order-based model for the kinetics of formation of Pickering emulsions. J. Colloid Interface Sci. 628, 409–416.
Tadros, T., 2013a. Encyclopedia of Colloid and Interface Science. Springer, Berlin, Heidelberg.
Tadros, T.F., 2013b. Emulsion Formation, stability, and rheology. In: Emulsion Formation and Stability. Wiley-VCH Verlag GmbH & Co. KGaA.
Taylor, G.I., 1934. The Formation of emulsions in definable fields of flow. Proc. Roy. Soc. Lond. A 146 (858), 501–523.
Tcholakova, S., Denkov, N.D., Sidzhakova, D., Ivanov, I.B., Campbell, B., 2003. Interrelation between drop size and protein adsorption at various emulsification conditions. Langmuir 19, 5640–5649.
Tcholakova, S., Denkov, N.D., Danner, T., 2004. Role of surfactant type and concentration for the mean drop size during emulsification in turbulent flow. Langmuir 20, 7444–7458.
Torza, S., Cox, R.G., Mason, S.G., 1972. Particle motions in sheared suspensions XXVII. Transient and steady deformation and burst of liquid drops. J. Colloid Interface Sci. 38 (2), 395–411.
Tran, H.-P., Arangalage, M., Jørgensen, L., Passade-Boupat, N., Lequeux, F., Talini, L., 2020. Understanding frothing of liquid mixtures: a surfactantlike effect at the origin of enhanced liquid film lifetimes. Phys. Rev. Lett. 125, 178002.
Traykov, T.T., Ivanov, I.B., 1977. Hydrodynamics of thin liquid films. Effect of surfactants on the velocity of thinning of emulsion films. Int. J. Multiphas. Flow 3 (5), 471–483.
Vankova, N., Tcholakova, S., Denkov, N.D., Ivanov, I.B., Vulchev, V.D., Danner, T., 2007. Emulsification in turbulent flow: 1. Mean and maximum drop diameters in inertial and viscous regimes. J. Colloid Interface Sci. 312 (2), 363–380.
Velikov, K.P., Velev, O.D., Marinova, K.G., Constantinides, G.N., 1997. Effect of the surfactant concentration on the kinetic stability of thin foam and emulsion flms. J. Chem. Soc., Faraday T rans. 93 (11), 2069–2075.

Verma, A., Kumar, N., Raj, R., 2020. Direct prediction of foamability of aqueous surfactant solutions using property values. article (in press) MOLLIQ-114635 J. Mol. Liq.
Voulgaropoulos, V., 2017. Dynamics of Spatially Evolving Dispersed Flows. Department of Chemical Engineering, University College London, PhD thesis.
Vrij, A., 1966a. Possible mechanism for the spontaneous rupture of thin, free liquid films. Discuss. Faraday Soc. 42, 23.
Vrij, A., 1966b. Possible mechanism for the spontaneous rupture of thin free liquid films. Discuss. Faraday Soc. 42, 23–33.
Wang, C.Y., Calabrese, R.V., 1986. Drop breakup in turbulent stirred-tank contactors. Part II: relative influence of viscosity and interfacial tension. AIChE J. 32 (4).
Wang, J., Yang, F., Tan, J., Liu, G., Xu, J., Sun, D., 2009. Pickering emulsions stabilized by a lipophilic surfactant and hydrophilic platelike particles. Langmuir 26, 5397–5404.
Ward, A.F., Tordai, L., 1946. Time-dependence of boundary tensions of solutions I. The role of diffusion in time-effects. J. Chem. Phys. 14, 453.
Yang, X., Verruto, V.J., Kilpatrick, P.K., 2007. Dynamic Asphaltene–Resin exchange at the oil/water interface: time-dependent W/O emulsion stability for asphaltene/resin model oils. Energy Fuel. 21 (3), 1343–1349.
Zhang, H.-Q., Sarica, C., 2006. Unified modeling of gas/oil/water pipe flow - basic approaches and preliminary validation. SPE Proj. Facil. Constr. 1 (2), 1–7.
Interfacial rheology of asphaltenes at oil-water interfaces and interpretation of the equation of state. Langmuir 29 (15), 2013, 4750–4759.